博　士　論　文

Collective Properties of Earthquakes and Active Faults

（地震と活断層の集団的性質）

Kazuyoshi Nanjo

平成12年

①

Doctoral Dissertation

2000

Collective Properties of Earthquakes and Active Faults

(地震と活断層の集団的性質)

Kazuyoshi Nanjo

(楠城一嘉)

Institute of Geology and Paleontology

Graduate School of Science

Tohoku University

Abstract

Earthquake phenomena seem to be complex. In complex systems, in general, one cannot reach the understanding of phenomena by a reductional description of simple elements or simple elementary processes, and mutual relationships of elements play important roles in determining the behavior of the whole system. Therefore, earthquake phenomena have to be understood by studying many earthquakes as an ensemble. Here, I study the collective properties of earthquakes and active faults.

The rate of aftershock decay is described by a power-law form (the modified Omori formula). The cumulative number of magnitudes of earthquakes satisfies an empirical relation known as the Gutenberg-Richter relation. The spatial distributions of given earthquakes show the scale-invariant behavior expressed by a power-law relation. The fracture systems including fault systems are statistically self-similar through the concept of fractal geometry. Here, I show the validity of these collective properties, for aftershock sequences following main shocks occurring in Japan and active fault systems within their aftershock regions. They are evidence of earthquakes of self-organized critical (SOC) phenomena.

Previous studies pointed out that internal structures and discontinuities in the lithosphere seem to influence on earthquakes. Here I examine the relationship between the fractal dimensions of aftershock spatial distribution and of pre-existing fracture systems, using observable data of aftershocks and active fault systems in Japan. The estimated fractal dimensions derive a positive correlation, showing that the aftershock distributions become less clustered with increasing the fractal dimensions of active fault

system. Therefore clustering aftershocks are constrained by the fractal properties of pre-existing active fault systems.

I develop my studies on the spatial distributions of aftershocks, considering the aftershock magnitudes. I observe the spatial distributions of the magnitude of aftershocks following shallower earthquakes in Japan. The upper limit of the aftershock magnitude is examined as a function of the distance from the main-shock hypocenter. The observed spatial distributions of the upper limit are bimodal, with a tendency of the upper limit to decrease as the distance from the main-shock hypocenter increases. Moreover, I correlate between the aftershock spatial distribution and earthquake fault length. I focus on the largest aftershocks in each of the two aftershock sequences constituting the bimodal distribution. The distances of the two largest aftershocks from the main-shock hypocenter are equal to the fault lengths of shallow earthquakes in Japan and to the maximum earthquake fault lengths.

To evaluate the collective properties of earthquakes and active faults from the view point of the anisotropy and entropic heterogeneity, I introduce the concept of the symmetropy. Using the symmetropy allows us to establish the method to measure quantitatively the anisotropy and entropic heterogeneity of the spatial distributions of (micro)fractures in the rock fracture experiment and in the SOC model of earthquakes. Moreover, considering the consistencey of the entropy relaxation with the occurrences of earthquakes (avalanches) in the SOC state, the process of the entropy relaxation can be monitored quantitatively by the symmetropy.

Contents

Chapter 1

Introduction

Statistical seismology, which aims to understand the global features of earthquake phenomena by studying many earthquakes as an ensemble, was the main school in the classical seismology. During 1950's, modern seismology supplanted classical seismology. Modern seismology aimed to understand the physical and technological properties of earthquakes as an independent, physical phenomenon, by analyzing them quantitatively (Ito, 1992). There has been renewed interest in studying many earthquakes as an ensemble (e.g., Turcotte, 1992, 1997; Shimazaki and Nagahama, 1995; Bak, 1996; Nanjo *et al.*, 1998; Nanjo and Nagahama, 2000), because it is connected with a new trend of science, which is concerned with the study of complex phenomena. In complex systems, in general, one cannot reach the understanding of phenomena by a reductional description of simple elements or simple elementary processes. Mutual relationships of elements play important roles in determining the behavior of the whole system (Ito, 1992). This viewpoint shows that earthquake phenomena cannot be understood without studying many earthquakes as an ensemble. In this paper, according to Shimazaki and Nagahama (1995), I call the properties of many earthquakes or faultings as an ensemble 'collective properties'. Here, I study the collective properties of earthquakes and active faults.

The rate of aftershock decay is described by a power-law form called the modified Omori formula (e.g., Omori, 1894; Utsu, 1957, 1969, 1999; Mogi, 1962, 1967; Nanjo *et al.*, 1998; Nanjo and Nagahama, 2000). The cumulative number of earthquakes of a given magnitude satisfies an empirical relation known as the Gutenberg-Richter relation (e.g., Gutenberg and Richter, 1954; Utsu, 1961, 1969, 1999; Nanjo *et al.*, 1998; Nanjo and Nagahama, 2000). The spatial distributions of hypocenters (epicenters) of given earthquakes show the scale-invariant behavior expressed by a power-law relation (e.g., Kagan and Knopoff, 1978, 1980; Yoshida and Mikami, 1986; Guo and Ogata, 1995, 1997; Nanjo and Nagahama, 2000). The fracture systems including fault systems statistically have the self-similar structure characterized by a power law, over a wide range of size scale through the concept of fractal geometry (e.g., Hirata, 1989b; Turcotte 1992, 1997; Shimazaki and Nagahama, 1995; Nanjo *et al.*, 1998; Nanjo and Nagahama, 2000). So, in Chap. 2, I show these collective properties for aftershock sequences following Japan earthquakes (main shocks) and active fault systems within their aftershock regions.

There is scale-free phenomenon known in physics, that is, the critical phenomenon. Critical phenomena occur at phase transitions like the gas-liquid transition at the critical temperature and the magnetic transition (Stanley, 1971). Power-law behavior is the characteristic nature associated with critical phenomena. Bak and co-workers (e.g., Bak *et al.*, 1988, 1989; Bak, 1996) submitted the dynamical systems with spatial degrees of freedom naturally evolve into a self-organized critical (SOC) state. Flicker noise or $1/f$ noise can be identified with the dynamics of the critical state. The SOC model is studied as a model for earthquake occurrence (e.g., Bak and Tang, 1989; Ito and Matsuzaki, 1990). The results in Chap. 2 are taken as circumstantial evidence of earthquakes of self-organized critical phenomena.

Internal structures and discontinuities in the lithosphere seem to have an influence on earthquakes. Nagahama and Teisseyre (1998, 2000a,b) discussed the relationship

between the fractal properties of fracturing in the lithosphere and of the micromorphic continuum, which is the continuum with microstructure. In the SOC model of earthquakes, Ito and Matsuzaki (1990) took the process called entropy relaxation (Enya, 1901) describing that main shock disturbs strain distribution and the aftershocks occur to decrease the heterogeneity of the strain distribution in the crust, and derived successfully some scaling laws of earthquakes. However, they did not confirm the influence of the internal structures and the discontinuities in the crust on the earthquake occurrences. Therefore, it is necessary to explore the relationship between the fractal properties of the earthquakes and of the discontinuities in the lithosphere.

A theoretical study derived the modified Omori formula from a preliminary statistical model where aftershocks are produced by a random walk on a pre-existing fracture system (Hirata, 1986). Nanjo *et al.* (1998) pointed out that the aftershock activity on frequency decay against time is characterized by the fractal dimension of a pre-existing fault system. However, the relationship between the fractal dimension of aftershock spatial distribution and that of active fault system has not been examined. If a relationship between them is found, one can demonstrate that each cluster of the aftershocks shows the fractal properties under the constraints of the fractal structure of the active fault systems. Here, in Chap. 3, I examine the relationship between the fractal dimensions of the epicentral distribution of fourteen aftershock sequences and the fractal dimensions of the pre-existing active fault systems within their aftershock regions, after reviewing the results of Nanjo *et al.* (1998). Finally, I discuss the fractal properties of aftershocks.

Several researchers have studied the distance between the main shocks and their largest aftershocks. The distances between the largest aftershocks and the main shocks occurring in Japan correlate positively to the main-shock magnitudes and to earthquake fault lengths (Hosono and Yoshida, 1991). For southern California earthquakes, one study has suggested that there might be two seismically characteristic distances from the main-shock epicenter where the largest aftershocks tend to occur (Hough and Jones,

1997). These results suggest a possible relationship between aftershock magnitudes and the rupture length of the main shock. However, a large earthquake can have several aftershocks large enough to cause damage, in contrast with the previous concern only about the largest aftershock in each aftershock sequence (Hosono and Yoshida, 1991; Hough and Jones, 1997). Thus, I seek to clarify the spatial distribution of magnitudes of all aftershocks as a function of the distance from the main-shock epicenter or hypocenter, focusing on the upper limits of the aftershock magnitude, and correlate such spatial distribution with earthquake fault lengths. Note that each aftershock in the spatial distributions considered here is regarded as a point with magnitude, by contrast with Chaps. 2 and 3, where each aftershock is regarded as a point without considering aftershock magnitude. In Chap. 4, I develop my studies on spatial distributions of aftershocks, considering the aftershock magnitudes. I examine the relationships between the aftershock magnitude and the hypocentral distance from the main shock to aftershocks following the six earthquakes of focal depth shallower than 20 km with magnitude more than 5.0 from 1983 to 1987 in Japan. Moreover, the observed spatial distributions of aftershocks are investigated by associating with earthquake fault lengths. Finally, I discuss earthquake fault length and Båth's law (Richter, 1958) which states that magnitude of the largest aftershock plus constant of 0.1 to 3 with an average value of 1.2, equals main-shock magnitude.

In the SOC model of earthquakes, Ito and Matsuzaki (1990) derived successfully some scaling laws of earthquakes, employing the process of the entropy relaxation (Enya, 1901) that is different from that of energy relaxation in the SOC model of Bak and Tang (1989). However, Ito and Matsuzaki (1990) have never measured the entropic heterogeneity of a system and discussed quantitatively the entropy relaxation.

Nanjo *et al.* (1998) pointed out that natural fracture systems in the 3-D crust are self-affine (anisotropic) rather than self-similar (isotropic). Moreover, other researchers have investigated self-affinity of microcrack systems in tensile laboratory tests of double torsion (Hatton *et al.*, 1993) and self-affine growth of earthquake rupture zones (Hatori,

1963; Nagahama, 1994b). No one has had the method to measure the quantitative anisotropy of fracture systems.

Mathematical group theory provides a very good tool to deal with perfect symmetries (Sattinger, 1978), but there is no perfect symmetry in nature. Thus, it is natural to analyze symmetry properties in terms of a continuous scale rather than in terms of 'yes or no' (e.g., Curie, 1894; Van Valen, 1962; Eigen and Winkler; 1975; Yodogawa, 1982; Palmer, 1986; Palmer and Strobek, 1986; Nagy, 1990, 1996; Zabrodsky *et al.*, 1992; Nanjo *et al.*, 2000). 'Unitary principle (Whyte, 1949a,b, 1974)' stated that 'asymmetry tends to disappear and this tendency is realized in isolable processes'. Dingle (1949) have described that 'the principle that nothing can be created or destroyed would have been disastrous to sciences, for it would have prohibited the conception of entropy, yet conservation laws are of the greatest value in restricted fields'. Moreover, Caillois (1973) submitted the tendency converse to the unitary principle, connecting with negentropy. These studies (Whyte, 1949a,b, 1974; Dingle, 1949; Caillois, 1973) propose that symmetry associates with entropy.

Yodogawa introduced 'symmetropy (Yodogawa, 1982; Nanjo *et al.*, 2000)' that mathematically connects between symmetry and entropy though information theory. It is a continuous measure to evaluate the anitropic and entropic heterogeneity of a given pattern and is satisfied with the previous proposition (Whyte, 1949a,b, 1974; Dingle, 1949; Caillois, 1973). However, no one has applied it to a pattern in nature. This symmetropy may be useful to monitor the spatial distributions of earthquakes or (micro)fracturing events, and provide a new measure to evaluate collective properties of earthquakes and active faults. In contrast with Chaps. 2 and 3, where the collective properties of earthquakes and active faults are studied from the viewpoint of isotropy, in Chap. 5 they are studied from the viewpoint of anisotropy and moreover entropic heterogeneity. Here, I introduce the concept of symmetropy. Next I examine the symmetropy of the spatial distributions of acoustic emissions generated by the microfracturing events in the laboratory experiment carried out by Hirata *et al.* (1987).

Moreover, I apply the symmetropy to the spatial patterns of earthquakes in the SOC model for fracturing (e.g., Bak and Tang, 1989; Bak, 1996; Jensen, 1998; Turcotte, 1999). Finally I discuss the symmetropies in the rock fracture experiment and in the SOC.

Chapter 2

Fractal properties of earthquakes and active faults

"No pain, no gain"

2-1. Fractal properties of earthquakes and active faults, and their characteristic exponents

I describe the modified Omori formula, the Gutenberg-Richter relation, the spatial distribution of earthquakes, and the fractal structure of fracture systems, with their characteristic exponents and the determination techniques of the fractal dimensions.

The decay of aftershock event rate $n(t)$ with time t was initially found to obey a simple hyperbolic law known as the Omori law (Omori, 1894). More generally Utsu (1957) showed that the rate of aftershock decay could be described by a power law, of the form:

$$n(t) \propto t^{-p}, \quad (1)$$

where p is a rate constant of aftershock decay and characterizes the mode of aftershock decay with time on frequency. Eq. 1 is called the modified Omori formula (Utsu, 1957). The Omori law is equivalent to the modified Omori formula with exponent $p = 1$. Eq. 1 implies that the relaxation function for aftershock activities on frequency shows a temporal fractal property, generally speaking, called a long time tail (Takayasu, 1990). Ogata (1988), studying statistical models for seismicity, found that an epidemic model, in which every earthquake can produce its aftershocks, fits better to the seismicity data than the restricted trigger model in which only main shocks can stimulate the aftershock occurrence. Aftershock sequences following the modified Omori formula were observed for acoustic emissions (AEs) in laboratory experiments (e.g., Scholz, 1968; Hirata, 1987). Several researches have empirically shown that the p-values of large earthquakes were close to 1 but ranged from 0.6 to 2.5 (e.g., Mogi, 1962, 1967; Utsu, 1969, 1999; Kisslinger and Jones, 1991; Guo and Ogata, 1995, 1997; Nanjo *et al.*, 1998; Wiemer and Katsumata, 1999; Nanjo and Nagahama, 2000). Systematic spatial distributions of the p-values of large earthquakes in and around Japan have been observed, where the p-values are less than 1.3 on the Pacific side, with above 1.3 on the side of the Sea of Japan (Mogi, 1962, 1967). However, it is not clear why each aftershock sequence has a significant different p-value. One reason may be the multifractal nature of seismicity (Main, 1996). Several theoretical studies have attempted to explain the Omori law and the modified Omori formula (Utsu, 1962, 1970; Scholz, 1968; Ohtsuka *et al.*, 1985; Hirata, 1986; Yamashita and Knopoff, 1987; Bak *et al.*, 1988; Ito and Matsuzaki, 1990; Shaw, 1993; Koyama, 1994, 1997). In particular, Hirata (1986) derived the modified Omori formula from a preliminary statistical model where aftershock sequences were produced by a random walk on a pre-existing fault system with an ideal fractal structure. This study implies that the p-value may be related to the fractal dimension of the pre-existing fault system in an aftershock region. Moreover, Hirata (1987) predicted

that the p-value decreases systematically as the fracture process advances on the basis of the experimental results with AEs following some bursts under uniaxial constant compression in basalt. If the model of Hirata (1986) and the above-mentioned prediction (Hirata, 1987) are correct, then the p-value gives quantitative information about fractal property of pre-existing fault system in the crust. Guo and Ogata (1995, 1997) studied the relationship between the p-values and the fractal dimensions of aftershock epicentral distribution in 2-D, not of pre-existing fault system. However, to our knowledge, the relationship between the p-values and the fractal dimensions of pre-existing surface-mapped fault systems has never been directly examined.

The number of earthquakes $N(M)$ with magnitudes greater than M satisfies an empirical relation known as the Gutenberg-Richter relation, given by:

$$\log N(M) = a - bM, \tag{2}$$

where a and b are constants (Gutenberg and Richter, 1954). The b-values are normally close to 1 but vary between 0.5 and 1.5. The Gutenberg-Richter relation holds for elastic shocks accompanying fractures of various materials (e.g., Mogi, 1962). It has been shown that this relation also holds for aftershock sequences (e.g., Utsu, 1961, 1969, 1999, Malin *et al.*, 1989). It has also been reported that there was a positive correlation with large scatter (Utsu, 1961; Guo and Ogata, 1995, 1997), and no correlation (Kisslinger and Jones, 1991) between the p- and the b-values for aftershock sequences from natural observable data. Utsu (1961) theoretically proposed a positive relation, $b = (2/\beta)\ p$ based on a model of residual strain energy of aftershock volume, where the constant β is 1.5, which is the slope of the log-linear relation between the total energy in the seismic waves generated by an earthquake and its magnitude. On the other hand, Ohtsuka *et al.* (1985) derived a negative relation, $b = 3 - 1.5p$, from introducing the modified Omori formula as a result of superposition of gamma decay functions. Then

Mikumo and Miyatake (1979) developed a frictional fault model with non-uniform strength, which exhibited a negative correlation between the *p*- and *b*-values. However, none of these explains the cause of observed scatter in the data. Several authors have noted that the *b*-values are also related to the fractal dimensions of size distribution or roughness of fracture (e.g., Caputo, 1976; Aki, 1981; King, 1983; Main and Burton, 1984; Turcotte, 1986a,b, 1989; Huang and Turcotte, 1988; Main *et al.*, 1989, 1990; Dubois and Novaili, 1989; Nagahama, 1991; Hatton *et al.*, 1993; Nagahama and Yoshii, 1994, Nagahama, 2000). In particular, Nagahama and Yoshii (1994) found that the fractal dimension of roughness of fracture in a 3-D medium is related with the *b*-value. Therefore the correlation and scatter between the *p*- and *b*-values are expected to give us information about geometry of fault system beneath the surface.

The spatial distributions of given earthquakes (e.g., regional seismicity and aftershocks) in the earth's crust and of AEs in rock specimen show scale-invariant (fractal; Mandelbrot, 1983) behavior (e.g., Kagan and Knopoff, 1978, 1980; Sadovisky *et al.*, 1984; Yoshida and Mikami, 1986; Hirata, 1989a; Hirata *et al.*, 1987; Guo and Ogata, 1995, 1997; Oncel *et al.*, 1995; Nanjo and Nagahama, 2000). For example, Kagan and Knopoff (1980) analyzed worldwide and local catalogues of earthquakes by using correlation functions (Grassberger, 1983) and presented self-similarity of earthquakes in the scale range from 0 to 2000 km. Analysis of spatial distributions of clustering aftershocks using the correlation integral (Grassberger, 1983) also exhibits scale-invariant behavior. The fractal dimensions of the aftershock spatial distributions for Japan earthquakes have been reported ranging from 1.9 to 2.9 for hypocenters (Yoshida and Mikami, 1986; Guo and Ogata, 1995, 1997) and ranging from 1.6 to 2.0 for epicenters (Nanjo and Nagahama, 2000). Yoshida and Mikami (1986) analyzed the aftershock sequence of the 1984 Nagano-ken Seibu earthquake in Japan, and reported the fractal behavior of the time-spatial distributions. Moreover, it was shown that the fractal properties were not changed by varying the lower limit of the magnitude of

aftershocks used in fractal analyses. Hirata *et al.* (1987) found that the spatial distributions of AE, which occurred during creep before ultimate whole fracture, show fractal structures, and the fractal dimensions decrease with the microfracturing.

Here, I introduce the two-point correlation integral $C(l)$ often used to evaluate a structure of a point collection (e.g., earthquakes, AE and galaxy) distributed in a space (Mandelbrot, 1983). $C(l)$ is defined as:

$$C(l) = \frac{1}{T^2} \sum_{i \neq j} F(l - R), \tag{3}$$

where T is the total number of points (earthquakes), $R = \| \bar{x}_i - \bar{x}_j \|$ is a distance between position vectors $\bar{x}_i$ and $\bar{x}_j$ of points, and $F(z)$ is the Heaviside function, which is 1 when $z \geq 0$, and is 0 when $z < 0$. If a point collection has a scale-invariant structure, then $C(l)$ is represented by a power-law form, given by:

$$C(l) \propto l^{D_2}, \tag{4}$$

where D_2 is defined as the fractal dimension (correlation dimension), which gives the lower limit of the Hausdorff dimension (e.g., Grassberger, 1983; Mandelbrot, 1983). D_2 provides a measure of degree of fractal clustering of points in a space, with lower fractal dimensions indicating tighter clusters (e.g., Hirata *et al.*, 1987; Nanjo and Nagahama, 2000). If a point distribution is completely random and unpredictable in a two-dimensional space, D_2 is 2. When $C(l)$ is evaluated for epicentral distribution of earthquakes, R between two given earthquakes must be defined. One often assumes that epicenters lie on the surface on a unit sphere. R (degree) is calculated by using a spherical triangle (e.g., Hirata, 1989a; Oncel *et al.*, 1995; Nanjo and Nagahama, 2000),

given by:

$$R = \cos^{-1}\left\{\cos\theta_1 \cos\theta_2 + \sin\theta_1 \sin\theta_2 \cos(\omega_1 - \omega_2)\right\}, \quad (5)$$

where (θ_1, ω_1) and (θ_2, ω_2) are north latitude (deg.) and east longitude (deg.) of two given epicenters.

The fracture systems including fault systems statistically have a self-similar structure over a wide range of size scale through the concept of fractal geometry introduced by Mandelbrot (1983) and extended by Turcotte (1992, 1997). As a consequence, fracture systems are characterized by a power law, with a characteristic exponent called a fractal dimension (e.g., Barton and Larsen, 1985; Scholz and Aviles, 1986; Watanabe, 1986; Aviles *et al.* 1987; Hirata, 1987; Okubo and Aki, 1987; Hirata, 1989b; Merceron and Velde, 1991; Velde *et al.*, 1991; Shimazaki and Nagahama, 1995; Nanjo *et al.*, 1998; Nanjo and Nagahama, 2000). For example, Okubo and Aki (1987) and Aviles *et al.* (1987) showed that the San Andreas fault systems possess self-similarity with fractal dimensions, using the ruler method and the method of covering a fault trace by circles, respectively. Hirata (1989b) and Shimazaki and Nagahama (1995) reported that active fault systems in Japan also possess self-similarity with fractal dimensions D_0 of 0.5 to 1.6, using the box-counting method. Both works pointed out a systematic change of D_0, which generally decreases with distance from the center in the Japan arc. On the other hand, Hatori (1963) pointed out that the aftershock regions, which are regarded as fracture zones, are elongated anisotropically as the magnitude of earthquake (main shock) increases. Moreover, non-self-similarity (self-affinity) of fractures or earthquakes has also been studied (Hatton *et al.*, 1993; Nagahama, 1994b). Nagahama (1994b) studied a self-affine growth pattern (anisotropic growth pattern) of earthquake rupture zones. Hatton *et al.* (1993) implied in tensile laboratory tests that fractal scaling of fracture system in specimens is self-affine.

Here I introduce the box-counting procedures (e.g., Korvin, 1992) often used to demonstrate self-similarity of fault geometry (e.g., Hirata, 1989b; Nanjo *et al.*, 1998; Nanjo and Nagahama, 2000). The fractal dimension measured by the box-counting method is called 'box-count dimension' in a practical sense, and is equivalent to 'capacity dimension' in a mathematical sense, usually denoted by D_0 (e.g., Korvin, 1992). D_0 can be used to quantify the occupancy rate of a fractal pattern in a space. Therefore, D_0 estimated for a fracture system characterizes the roughness of fracture or the occupancy of fracture system (Nanjo *et al.*, 1998; Nanjo and Nagahama, 2000). Supporting this quantitatively, a positive correlation of D_0 with the length of active fault lines per unit area (density of active faults) is also ascertained (Shimazaki and Nagahama, 1995). The box-counting procedure used for fracture systems is given below: An active fault system in a given extent (aftershock region in this study) is overlaid with a grid of square boxes; grids of different size boxes are used. The aftershock region thus must be rectangle. The number of boxes $N(r)$ of size r required to cover the fault system is plotted on a double-logarithmic graph as a function of r. If the active fault system has a self-similar structure, then we derive the following relationship,

$$N(r) \propto r^{-D_0}, \tag{6}$$

where D_0 is defined as the fractal dimension (box-counting dimension or capacity dimension).

2-2. Data and definitions of aftershocks and aftershock region

I present that aftershock sequences and active fault systems within their aftershock

regions are satisfied with the modified Omori formula, the Gutenberg-Richter relation, the fractality of spatial distribution of earthquakes and the fractal structure of fracture systems. Natural data of seismicity and fault systems are required for such presentation.

I use the two data source of earthquakes: the file 'SEIS-PC' (Ishikawa, 1986; Ishikawa *et al.*, 1989), in which data of earthquakes occurring in and around Japan since 1885 are listed (original data are from Japan Meteorological Agency), and the earthquake catalogue of the Disaster Prevention Research Institute (DPRI) of Kyoto University. These comprise data on aftershock sequences following fifteen main shocks of magnitude $M_M \geq 5.2$ from 1931 to 1995 in Japan (Table 1). SEIS-PC is used for fourteen of the aftershock sequences used here. The earthquake catalogue of DPRI is used for the aftershock sequence of the 1995 Hyogo-ken-nanbu earthquake, because SEIS-PC has no data sets of earthquakes after 1993 and the DPRI catalogue comprised data for up to dozens of days following the 1995 Hyogo-ken-nanbu earthquake.

Errors of the epicentral locations and depth of earthquakes in 1930-1940's are more or less ± 1' and ± 10 km, respectively. Errors of them in 1960-1970's are more or less ± 1' and ± 5 km, respectively. Errors of them in 1980-1990's are more or less ± 0.1' and ± 1 km, respectively. Earthquakes with magnitude $M \geq 0$ are treated in present analyses. $M = 0$ is the lowest magnitude in the both data sets. The earthquake data of SEIS-PC and DPRI used in my analyses show detection confidence for whether an earthquake event occurred at that time, although they may be doubtful for low-magnitude values (maybe of 0 to 2). In order to make a population of analyzed data, cutoff magnitude should be set down as small as possible. That is why the cutoff magnitude is 0.

The data on active faults are from 'Active Faults in Japan' (The Research Group for Active Faults of Japan, 1991), which consists of map sheets of active faults on a scale of 1:40,000. In this book, active faults are defined as faults which were active during Quaternary (2 Ma to the present) and may possibly move again soon. The listed active faults on land were identified by careful interpretation of air photographs and

Table 1 Earthquake origins of 15 main shocks followed by analyzed aftershock sequences and the estimated values of p and b. Loc: location (north latitude, east longitude) (deg.); Dep: focal depth (km); M_M: magnitude, of main shocks. Main data source of the earthquakes is from 'SEIS-PC' (Ishikawa, 1986; Ishikawa *et al.*, 1989). Earthquake data source of Hyogo-ken Nanbu earthquake is from the Disaster Prevention Research Institute of Kyoto University. Data on active faults are from 'Active Faults in Japan' (The Research Group for Active Faults of Japan, 1991). Some older earthquakes have a lower reliability of the depth value, presented by '-' in the column Dep. Values in the parentheses are error bounds.

Main shock	Date	Loc	Dep	M_M	p	b
Nishisaitama earthquake	1931.9.21	(36.2, 139.1)	-	6.9	1.13 (0.02)	0.85 (0.01)
Tottori earthquake	1943.9.10	(35.5, 134.1)	-	7.2	1.19 (0.04)	0.79 (0.01)
Mikawa earthquake	1945.1.13	(34.7, 137.1)	-	6.8	1.08 (0.04)	0.89 (0.01)
Fukui earthquake	1948.6.28	(36.2, 136.2)	-	7.1	1.07 (0.02)	0.85 (0.00)
Imaichi earthquake	1949.12.26	(36.6, 139.8)	-	6.4	1.10 (0.02)	0.91 (0.05)
Kitamino earthquake	1961.8.19	(36.0, 136.8)	-	7.0	1.13 (0.04)	0.65 (0.03)
Central Gifu Prefecture	1969.9.9	(35.8, 137.1)	-	6.6	1.08 (0.03)	0.87 (0.01)
Eastern Yamanashi Prefecture	1976.6.16	(35.5, 139.0)	-	5.5	1.06 (0.01)	0.89 (0.01)
Boundary between Kanagawa and Yamanashi Prefectures	1983.8.8	(35.5, 139.0)	18	6.0	1.06 (0.04)	0.87 (0.00)
Eastern Tottori Prefecture	1983.10.31	(35.4, 133.9)	15	6.2	1.20 (0.05)	0.77 (0.01)
Near Unzen	1984.8.6	(32.8, 130.2)	7	5.7	0.93 (0.03)	1.30 (0.01)
Nagano-ken Seibu earthquake	1984.9.14	(35.8, 137.6)	2	6.8	1.01 (0.02)	0.97 (0.00)
Northern Nagano Prefecture	1986.12.30	(36.6, 137.9)	3	5.9	1.18 (0.07)	0.64 (0.01)
Yamaguchi Prefecture	1987.11.18	(34.1, 131.5)	8	5.2	1.21 (0.02)	0.59 (0.03)
Hyogo-ken Nanbu earthquake	1995.1.17	(34.6, 135.0)	18	7.2	0.67 (0.01)	0.63 (0.00)

were confirmed by land survey. This research group classified all faults mapped in this book into three groups on the basis of the judgments as follows: (1) it is certain beyond doubt that the fault was active during the Quaternary; (2) it is not definitely certain that the fault was active during the Quaternary but it is possible to infer the sense of the displacement; and (3) a fault is a lineament (linear topography) suspected of being a fault active during the Quaternary. Irrespective of the classification, all active faults listed up were used in my analyses. Active submarine faults identified by seismic reflection profiles were also included when they are within the aftershock regions.

Aftershocks must be clearly distinguished from other background events. It is a serious problem in that the definition of an aftershock varies from one investigator to the other (Frohlich, 1989; Kisslinger, 1996). Following Utsu (1991), we define aftershock events as earthquakes in swarms around the main shock (large event), tentatively within the next 1000 days (Nanjo *et al.*, 1998; Nanjo and Nagahama 2000). In the present work fractal analyses are carried out for active fault systems within aftershock regions. For the convenience of treatment, the aftershock region is re-defined as the smallest rectangle in which all aftershock epicenters are included (Nanjo *et al.*, 1998; Nanjo and Nagahama 2000). Fig. 1 shows the spatial epicentral distribution of aftershocks (solid circles) following the Fukui earthquake (open circle). Fig. 2 shows the active faults (solid lines) in and around the aftershock region (surrounded by broken lines) of the Fukui earthquake.

The aftershock sequences following the Tottori earthquake and the earthquakes occurred in the eastern Tottori prefecture consist of the smallest and the second smallest numbers of aftershocks, respectively, in the twelve aftershock sequences.

2-3. Results and discussions

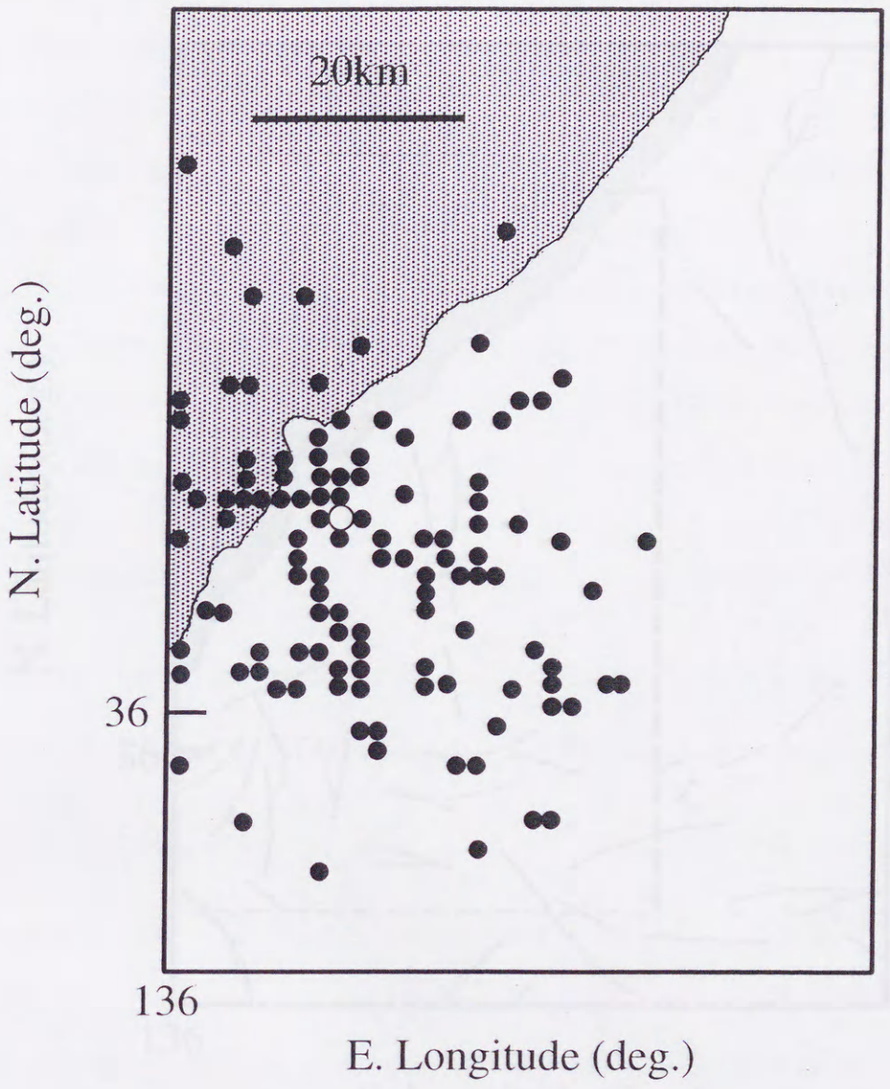

Fig. 1 Epicentral distribution of aftershocks following the Fukui earthquake. Open and solid circles are epicenters of the main shock and of aftershocks, respectively.

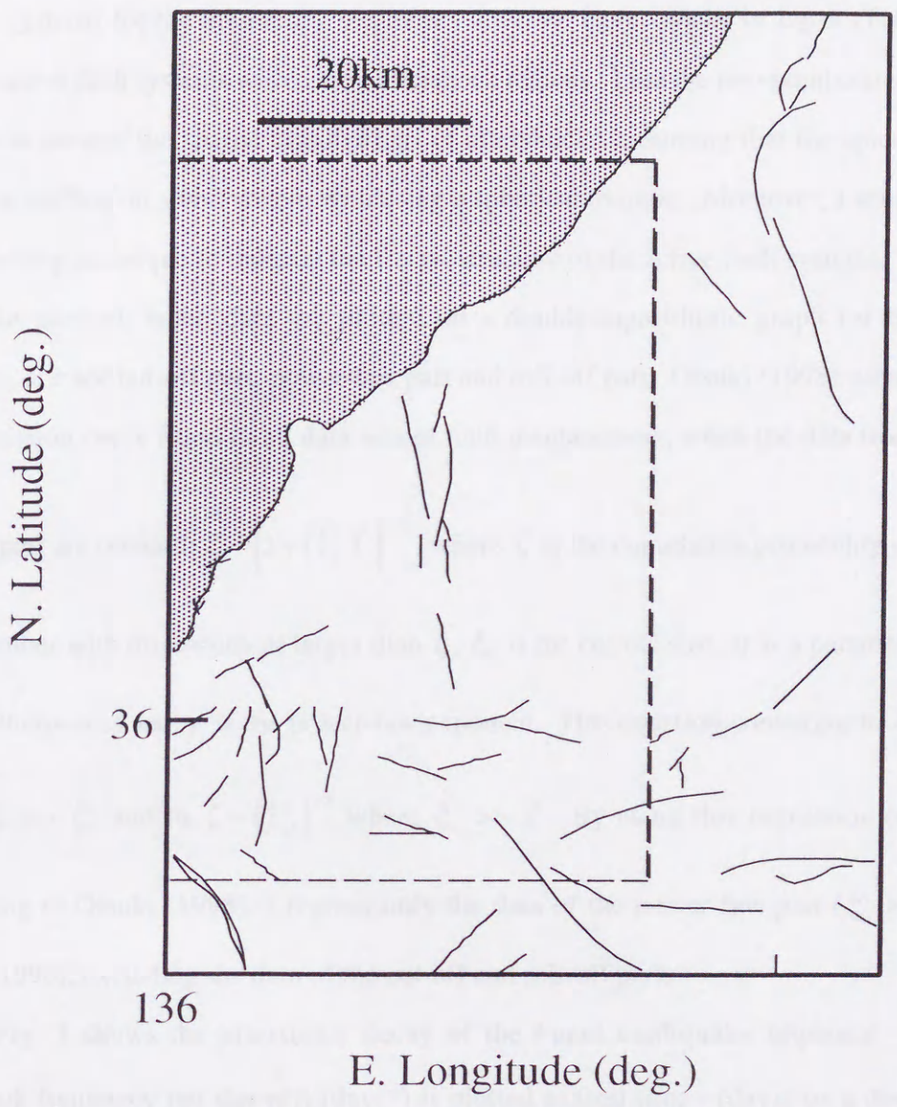

Fig. 2 Active faults in and around the aftershock region of the Fukui earthquake. Solid lines are active faults. The aftershock region is the rectangle surrounded by broken lines.

I show the modified Omori formula, the Gutenberg-Richter relation for aftershock sequences, the fractality of the spatial distribution of aftershocks, and the fractal structure of fault systems for the aftershock sequences after the main shocks in Japan (Table 1) and the active fault systems within their aftershock regions. I use the two-point correlation integral to present the spatial distributions of aftershocks, assuming that the epicenters lie on the surface on a unit sphere with using a spherical triangle. Moreover, I adopt the box-counting technique to indicate the fractal structure of the active fault systems.

In general, when data are plotted on a double-logarithmic graph for fractal analyses, one see cut-off part, power-law part and roll-off part. Otsuki (1998) submitted the regression curve fitted to all data sets of fault displacement, when the data from the roll-off part are omitted: $\zeta = \left[1 + \left(\xi / \xi_C\right)^{\eta}\right]^{-\gamma/\eta}$, where ζ is the cumulative probability of the fault number with displacement larger than ξ, ξ_C is the cut-off size, η is a parameter of cut-off sharpeness and γ is the power-law exponent. This equation converges to $\zeta = 1$ where $\xi >> \xi_C$ and to $\zeta = \left(\xi / \xi_C\right)^{-\gamma}$ where $\xi_C >> \xi$. By using this regression curve, According to Otsuki (1998), I regress only the data of the power-law part ($\xi_C >> \xi$; Otsuki, 1998), excluding the data of the cut-off and roll-off parts.

Fig. 3 shows the aftershock decay of the Fukui earthquake sequence. The aftershock frequency per day $n(t)$ (days^{-1}) is plotted against time t (days) on a double-logarithmic graph. The results obey the modified Omori formula (Eq. 1) with $p = 1.07 \pm 0.02$, estimated from the slope of the regression line fitted to these data in the range $0.1 \leq t \leq 1000$ by the least-squares method. The other fourteen aftershock sequences also statistically obey this power-law decay. The p-values thus obtained are found to be in the range $0.66 \leq p \leq 1.25$ for the fifteen sequences. The estimated p-values are summarized in Table 1.

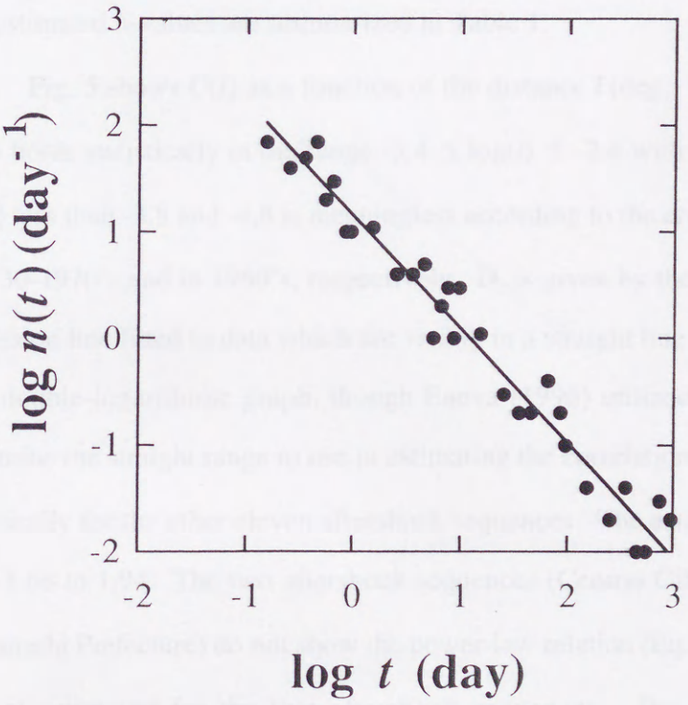

Fig. 3 Aftershock decay of the Fukui earthquake. Aftershock frequency per day $n(t)$ (day^{-1}) is plotted against time t (day) on a double-logarithmic graph. Aftershock frequency statistically obeys a power law (the modified Omori formula) with $p = 1.07 \pm 0.02$, the slope of the least-square regression line fitted to the data in the range $0.1 \leq t \leq 1000$.

Fig. 4 shows the size distribution of the aftershock sequence following the Fukui earthquake. The number of aftershocks $N(M)$ with magnitudes greater than M is plotted against magnitude M on a semi-logarithmic graph. Because we observe that at $M = 4.1$, the cumulative number of small events begins to fall off from the Gutenberg-Richter relation (Eq. 2), $b = 0.85 \pm 0.00$ of the Gutenberg-Richter relation is estimated from the slope of the least-square regression line fitted to the data in the range $4.1 \leq M \leq 4.9$. The other fourteen aftershock sequences also statistically obey the Gutenberg-Richter relation with the minimum magnitudes ranging from 1.5 to 4.1 in the analyses of the regressions. The b-values for the fifteen events are thus in the range $0.43 \leq b \leq 1.31$. The estimated b-values are summarized in Table 1.

Fig. 5 shows $C(l)$ as a function of the distance l (deg.) for the Fukui earthquake. Eq. 4 holds statistically in the range $-3.4 \leq \log(l) \leq -2.4$ with $D_2 = 1.82 \pm 0.00$. Here, $\log(l)$ less than -3.8 and -4.8 is meaningless according to the errors of epicenter locations in 1930-1970's and in 1980's, respectively. D_2 is given by the slope of the least-square regression line fitted to data which are visibly in a straight line within an observed range on a double-logarithmic graph, though Eneva (1996) utilized a different technique to determine the straight range to use in estimating the correlation dimensions. Eq. 4 holds statistically for the other eleven aftershock sequences. The estimated values of D_2 range from 1.68 to 1.94. The two aftershock sequences (Central Gifu Prefecture and Eastern Yamanashi Prefecture) do not show the power-law relation (Eq. 4). Therefore, D_2-values are not estimated for the two aftershock sequences. The estimated D_2-values are summarized in Table 2.

Fig. 6 shows the results of the fractal analysis of the active fault system in the aftershock region of the Fukui earthquake. Eq. 6 holds statistically in the range $1.7 \leq r \leq 33.3$ (km) with $D_0 = 1.09 \pm 0.01$. D_0 is given by the slope of the least-square regression line fitted to data within an range on a double-logarithmic graph. Eq. 6 holds statistically for the other fourteen active fault systems. The estimated values of D_0

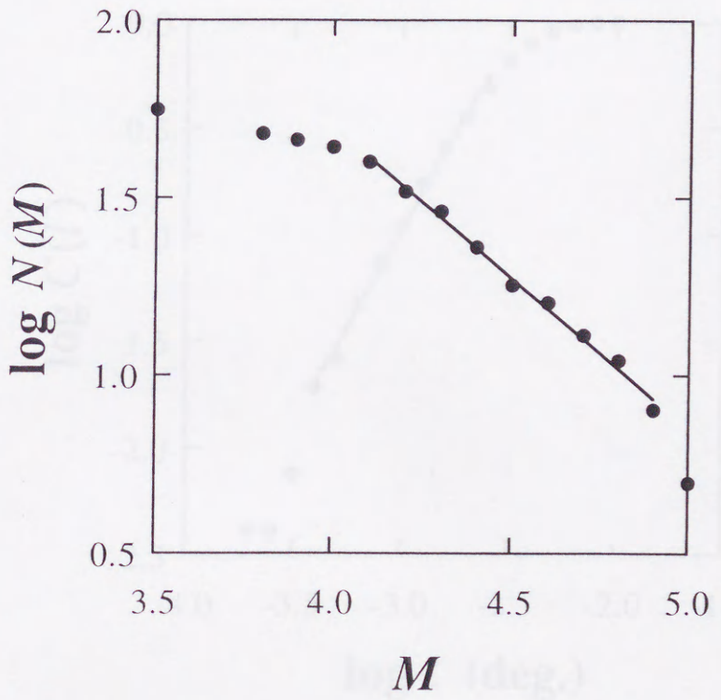

Fig. 4 Size distribution of aftershocks following the Fukui earthquake. The number of earthquakes $N(M)$ with magnitudes greater than M is plotted against M on a semi-logarithmic graph. Because we observe that at $M = 4.1$, the cumulative number of small events begins to fall off the Gutenberg-Richter relation (Malin *et al.*, 1989), $b = 0.85 \pm 0.00$ of the Gutenberg-Richter relation is estimated from the slope of the least-square regression line fitted to the data in the range $4.1 \leq M \leq 4.9$.

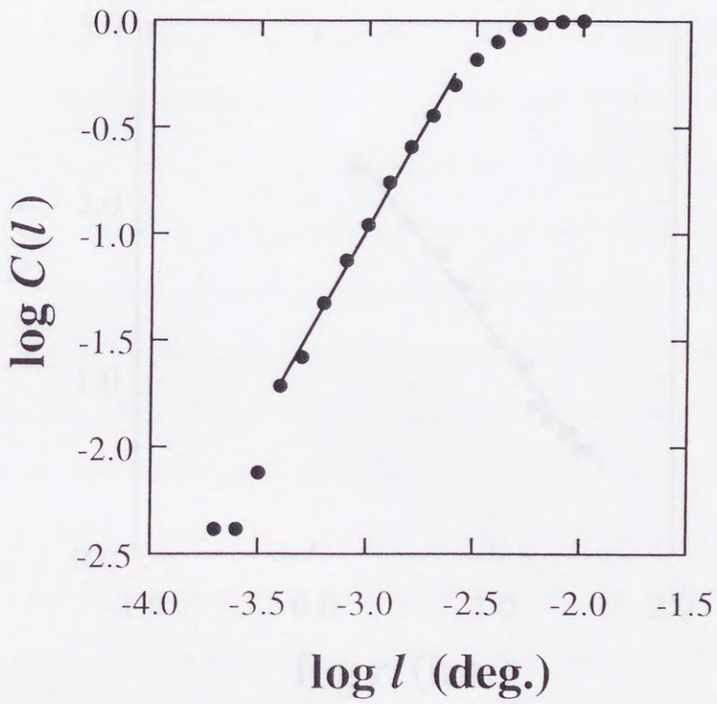

Fig. 5 Correlation integral $C(l)$ as a function of the distance l (deg.) for the Fukui earthquake. The estimated fractal dimension (D_2) is 1.82 ± 0.00, the slope of the least-square regression line fitted to these data in the range $-3.4 \leq \log(l) \leq -2.4$.

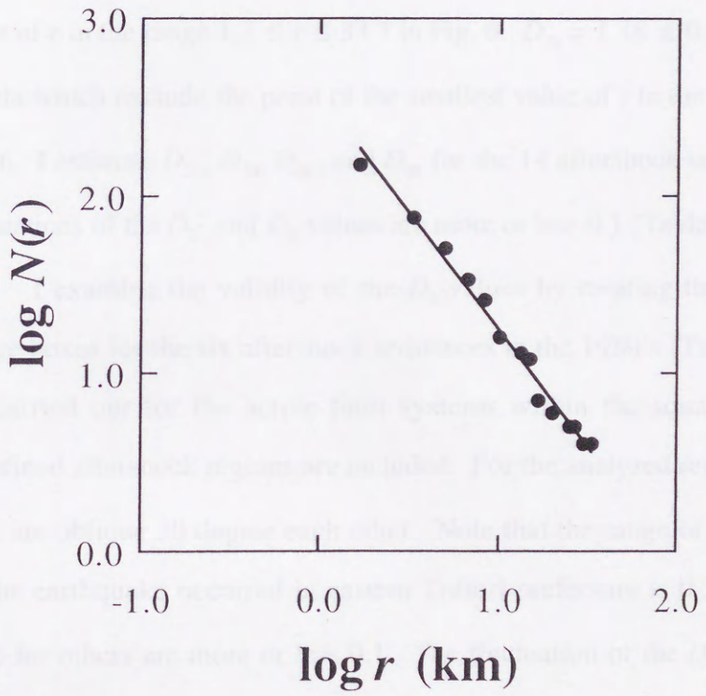

Fig. 6 Results of fractal analysis of the active fault system in the aftershock region of the Fukui earthquake. The number of boxes entered by the line of active faults $N(r)$ is plotted against the side length of square box r (km) on a double-logarithmic graph. The estimated fractal dimension (D_0) is 1.32 ± 0.01, the least-square regression line fitted to these data in the range $1.7 \leq D_0 \leq 33.3$ (km).

range from 0.86 to 1.48 and are summarized in Table 2.

I check the fluctuations of the D_2- and D_0-values by changing the range of the power-law part. For the aftershock sequence of the Fukui earthquake, $D_{2L} = 1.81 \pm 0.01$ is given by the slope of the least-square regression line fitted to data which exclude the point of the largest value of $\log(l)$ ($\log(l) = -2.4$) in the range $-3.3 \leq \log(l) \leq -2.4$ in Fig. 5. $D_{2S} = 1.87 \pm 0.00$ is given by that fitted to data which exclude the point of the smallest value of $\log(l)$ ($\log(l) = -3.3$) in the range $-3.3 \leq \log(l) \leq -2.4$ in Fig. 5. Similarly, for the active fault system within the aftershock region of the Fukui earthquake, $D_{0L} = 1.33 \pm 0.01$ is given by that fitted to data which exclude the point of the largest value of r in the range $1.7 \leq r \leq 33.3$ in Fig. 6. $D_{0S} = 1.38 \pm 0.01$ is given by that fitted to data which exclude the point of the smallest value of r in the range $1.7 \leq r \leq 33.3$ in Fig. 6. I estimate D_{2L}, D_{2S}, D_{0L}, and D_{0S} for the 14 aftershock sequences (Table 2). The fluctuations of the D_2- and D_0-values are more or less 0.1 (Table 2).

I examine the validity of the D_0-values by rotating the direction of a grid of square boxes for the six aftershock sequences in the 1980's (Table 3). Fractal analyses are carried out for the active fault systems within the square region in which the re-defined aftershock regions are included. For the analyzed region, the direction of the grids are oblique 30 degree each other. Note that the range of the estimated D_0-values for the earthquake occurred in eastern Tottori prefecture is 0.24, in contrast with that those for others are more or less 0.1. The fluctuation of the D_0-values are regarded to reflect the regional anisotropy of the fault geometry. This method may be important in order to examine the spatial anisotropy of active fault systems.

Mechanical property of rocks in the upper lithosphere is approximately elastic at low temperature (e.g., Ranalli, 1987). Thus brittle crust with fault systems has been considered analogous to a system governed by elastic equations (Laplace equations) which represent local balances of forces (e.g., Nakamura *et al.*, 1996). Moreover, Kagan (1992) and Otsuki (1998) pointed out the similarity of brittle fracturing to turbulent

Table 2 The estimated values of D_2, D_0, D_{2L}, D_{2S}, D_{0L}, and D_{0S}. For spatial distribution, Central Gifu prefecture and Eastern Yamanashi prefecture do not show scale invariance, and Hyogo-ken Nanbu earthquake is not used in this paper, indicated by '-' in the column D_2. Values in the parentheses are error bounds.

Main shock	D_2	D_{2L}	D_{2S}	D_0	D_{0L}	D_{0S}
Nishisaitama earthquake	1.70 (0.01)	1.70 (0.01)	1.68 (0.01)	1.09 (0.01)	1.10 (0.02)	1.16 (0.02)
Tottori earthquake	1.82 (0.01)	1.87 (0.01)	1.80 (0.01)	0.91 (0.01)	0.87 (0.01)	0.97 (0.02)
Mikawa earthquake	1.75 (0.00)	1.80 (0.00)	1.71 (0.00)	1.18 (0.01)	1.16 (0.01)	1.23 (0.01)
Fukui earthquake	1.82 (0.00)	1.87 (0.00)	1.81 (0.01)	1.32 (0.01)	1.33 (0.01)	1.38 (0.01)
Imaichi earthquake	1.69 (0.01)	1.77 (0.00)	1.66 (0.01)	1.14 (0.01)	1.10 (0.01)	1.20 (0.01)
Kitamino earthquake	1.79 (0.01)	1.87 (0.00)	1.76 (0.01)	1.22 (0.01)	1.24 (0.01)	1.22 (0.01)
Central Gifu Prefecture	-	-	-	1.21 (0.01)	1.24 (0.01)	1.20 (0.03)
Eastern Yamanashi Prefecture	-	-	-	1.30 (0.01)	1.30 (0.02)	1.40 (0.01)
Boundary between Kanagawa and Yamanashi Prefectures	1.84 (0.00)	1.89 (0.00)	1.82 (0.00)	1.28 (0.01)	1.31 (0.01)	1.33 (0.02)
Eastern Tottori Prefecture	1.75 (0.01)	1.80 (0.01)	1.76 (0.01)	0.86 (0.00)	0.85 (0.00)	0.87 (0.00)
Near Unzen	1.91 (0.00)	1.91 (0.00)	1.83 (0.00)	1.39 (0.01)	1.36 (0.01)	1.47 (0.01)
Nagano-ken Seibu earthquake	1.94 (0.00)	1.98 (0.00)	1.93 (0.00)	1.45 (0.01)	1.47 (0.01)	1.50 (0.01)
Northern Nagano Prefecture	1.77 (0.00)	1.83 (0.00)	1.77 (0.01)	1.17 (0.01)	1.16 (0.01)	1.24 (0.01)
Yamaguchi Prefecture	1.68 (0.00)	1.71 (0.00)	1.67 (0.00)	1.08 (0.00)	1.07 (0.01)	1.13 (0.00)

Table 3 The fluctuation of the D_0-values by rotating the direction of a grid of square boxes. For the analyzed region, the direction of the grids are oblique 30 degree each other.

Main shock	0 (deg.)	30 (deg.)	60 (deg.)	Fluctuation
Boundary between Kanagawa and Yamanashi Prefectures	1.34 (0.01)	1.25 (0.01)	1.24 (0.01)	0.12
Eastern Tottori Prefecture	1.02 (0.01)	0.87 (0.00)	0.79 (0.00)	0.24
Near Unzen	1.35 (0.00)	1.28 (0.00)	1.25 (0.00)	0.10
Nagano-ken Seibu earthquake	1.37 (0.01)	1.34 (0.01)	1.28 (0.01)	0.10
Northern Nagano Prefecture	1.09 (0.00)	1.07 (0.00)	1.14 (0.01)	0.08
Yamaguchi Prefecture	0.80 (0.01)	0.91 (0.00)	0.91 (0.00)	0.11

flow. Turbulent flow can be described by the Navier-Stokes equation. The Navier-Stokes equation for steady-state flow of a viscous fluid at low Reynolds number is equivalent to the Navier equation which is the generalization of Laplace equation (Nagahama and Teisseyre, 2000b). As shown in this chapter, I studied several fractal properties of faults and earthquakes, such as the Gutenberg-Richter relation (Eq. 2), which is a kind of dissipative structure (Hwa and Kadar, 1989; Otsuki, 1998). By considering the SOC model (e.g., Hwa and Karder, 1989; Bak, 1996), it was found that if the dynamics is satisfied with a local conservation law, then the steady configurations have to be fractal and the system is self-organized into criticality. Thus the results in this chapter are taken as circumstantial evidence that earthquakes are SOC phenomena (e.g., Bak and Tang, 1989; Ito and Matsuzaki, 1990).

In conclusions, aftershock sequences following earthquakes (main shocks) in Japan and active fault systems within their aftershock regions satisfy the modified Omori formula of aftershocks and the Gutenberg-Richter relation. Moreover, they show the fractal properties for the spatial distributions of epicenters and active faults. The fluctuations of the D_2- and D_0-values by changing the range of the power-law part are more or less 0.1. The range of the fluctuation of the D_0-values by rotating a square grid of the box-counting method for the earthquake occurred in eastern Tottori prefecture is 0.24, contrary to that those for others are more or less 0.1. The results in this chapter are taken as circumstantial evidence of earthquakes of SOC phenomena.

Chapter 3

Fractal properties of aftershock spatial distributions and active fault systems

"青出於藍而青於藍"

from 荀子, 勧学

3-1. Rates of aftershock decay and the fractal structure of active fault systems

For fifteen aftershock sequences following main shocks that occurred in Japan from 1931 to 1995 (Table 1), Nanjo *et al.* (1998) examined the relationship between the *p*-values and the fractal capacity dimensions D_0 of the pre-existing surface active-fault systems in the aftershock regions, and the relationship between the *p*- and *b*-values. In this work they used the seismicity data of the software 'SEIS-PC' (Ishikawa, 1986; Ishikawa *et al.*, 1989) and the earthquake catalogue of the Disaster Prevention Research Institute (DPRI) of Kyoto University to obtain the *p*- and *b*-values. In this procedure

they followed the phenomenological definition of aftershocks (Utsu, 1991), to separate aftershocks from other events in the data sources. They used 1:40,000 maps from the 'Active Faults in Japan' (The Research Group for Active Faults of Japan, 1991) to derive the D_0-values. In the paper they used the standard box-counting technique (Korvin, 1992). They obtained the estimated values of p, b and D_0 in the ranges $0.66 \leq p \leq 1.23$, $0.43 \leq b \leq 1.31$ and $0.85 \leq D_0 \leq 1.47$, respectively (Table 1). The p- and b-values of some aftershock sequences were different from those obtained in previous works (Mogi, 1962, 1967; Utsu, 1969; Guo and Ogata, 1995, 1997), because the seismicity data, the working definition of aftershocks (Frohlich, 1989), and the estimation technique for the p- and the b-values were different from those adopted in the earlier works. From the estimated values of p, b and D_0 in the paper, they observed: (1) a negative correlation and also some scatter between the p- and D_0-values with a regression line $D_0 = (-2.10 \pm 0.35)p + (3.50 \pm 0.38)$, and (2) a negative correlation and also some scatter between the p- and b-values with $b = (-2.45 \pm 0.53)p + (3.54 \pm 0.58)$. Observation (1) shows that the p-value decreases systematically with increasing the occupancy rate (roughness of fracture) of the pre-existing active fault system in the crust, and suggests that aftershock decay dynamics is constrained by pre-existing fracture system. Observation (2) shows that their data negate the theoretical equations of both $b = (4/3)p$ (Utsu, 1961) and $b = 3 - 1.5p$ (Ohtsuka *et al.*, 1985). They offered a possible interpretation on these negative correlations and some scatter in both observations; the scatters are interpreted as the scatter of the difference of two fractal dimensions between 3-D fracture construction in the crust and 2-D cross-sectional surface (observed active-fault system). This result strongly suggests that the scaling for a natural fracture system is self-affine (with different fractal scaling in different directions) rather than self-similar, which would be a manifestation of regional anisotropy of the fracture system. Further tests to examine the effect of the dips of the main-shock faults (Sato *et al.*, 1989) with fractal topography

(Brown and Scholz, 1985) on the self-affine scaling, show the rejection of the effect and support the suggestion.

3-2. Relationship between D_2 and D_0

Fig. 7 illustrates the relationship between the D_2-values of the spatial distribution of aftershocks and the D_0-values of the active fault system within the aftershock regions. Here the data of D_2 and D_0 are from Table 2 and the errors of them comes from D_2, D_{2L}, D_{2S}, D_0, D_{0L}, and D_{0S}. I separate the data according to the accuracy of the detection of earthquakes. Note that Nanjo *et al.* (1998) have never been examined the relationship between them. Excluding the points of the Tottori earthquake and the Eastern Tottori Prefecture, one can find a positive correlation with a least-square regression line given by:

$$D_2 = (0.72 \pm 0.02)D_0 + (0.91 \pm 0.02). \quad (7)$$

The two aftershock sequences are excepted from the regression, because the two points are far from the general tendency and have lower reliability than the others. The number of aftershocks in the excepted cases is not large enough to estimate D_2-values. As stated above in Chap. 2, the two aftershock sequences consist of the smallest and the second smallest numbers in the twelve aftershock sequences. Moreover, as shown in Chap. 2, the range of the estimated D_0-values (0.24) by rotating a square grid of the box-counting method for the earthquake occurred in eastern Tottori prefecture is much larger than those for others (more or less 0.1). The aftershock region of the Tottori earthquake is close to that of the earthquake occurred in eastern Tottori prefecture. That

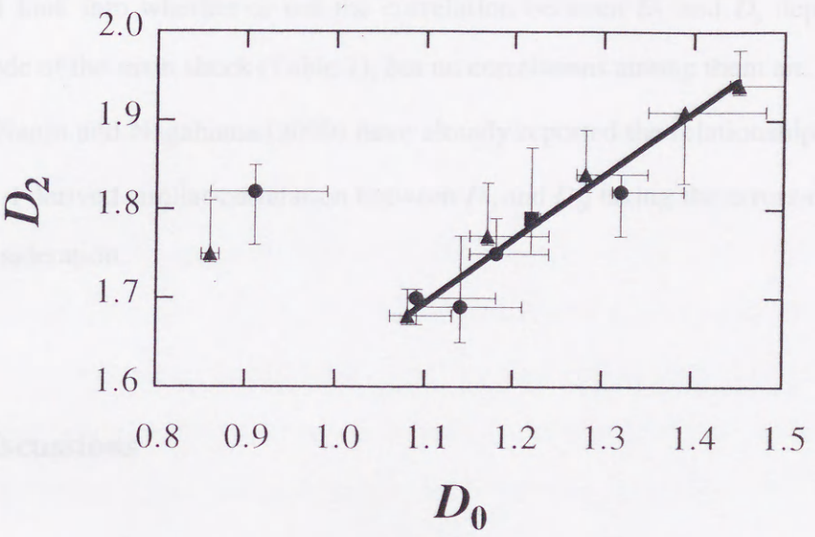

Fig. 7 The fractal dimensions (D_0) of the active fault system vs. the fractal dimensions (D_2) of epicentral distribution. Excepting the Tottori earthquake and Eastern Tottori prefecture, a positive correlation is found with the least-square regression line, $D_2 = (0.72 \pm 0.02)D_0 + (0.91 \pm 0.02)$. Circle, squuare, triangle represent the earthquakes occurred in 1930-1940's, 1970's and 1980's, respectively.

is why I exclude the points of the two earthquakes from the regression. When only the six data of 1980's are plotted, one see also a positive correlation between D_2 and D_0, excepting the data point of the earthquake occurred in eastern Tottori prefecture. The positive correlation indicates that the fractal clustering of aftershock distribution, D_2, becomes less strong with increasing D_0. The estimated D_2-values were less than 2 (Table 1). Eq. 7 means that the aftershocks tend to distribute more randomly with increasing the fractal dimensions of the active fault systems in the aftershock regions.

I look into whether or not the correlation between D_2 and D_0 depends on the magnitude of the main shock (Table 1), but no correlations among them are found.

Nanjo and Nagahama (2000) have already reported the relationship between D_2 and D_0. I derived similar correlation between D_2 and D_0, taking the errors of D_2 and D_0 into consideration.

3-3. Discussions

The estimated box-counting dimension of the active fault systems, D_0, ranges from 0.86 to 1.48 (Table 1). The upper limits of D_0 of fracture geometry in rock were reported to be nearly equal to 1.5 in a two-dimensional space (Hirata, 1989b; Nanjo *et al.*, 1998; Nanjo and Nagahama, 2000). Here note that the maximum value of D_0 in this paper is quite close to the upper limit of the fractal dimension $D_0 = 1.5$. If D_0 of the active fault system in this paper is equal to the upper limit of $D_0 = 1.5$, then D_2 is given to be quite close to 2.0 by Eq. 7. Actually, the maximum value of the estimated D_2 is 1.94. In the case of $D_2 = 2.0$ in a two-dimensional space, the clustering aftershocks exhibit a completely random distribution. However, the estimated D_0 ranging from 0.86

to 1.48 is correlated with the estimated D_2 ranging from 1.68 to 1.94 (Table 1). If D_0 is equal to zero, D_2 is given to be close to one. That is, each cluster of the aftershocks shows the fractal properties under the constraints of the fractal structure of the active fault systems.

Hirata (1986) derived the modified Omori formula from a model in which aftershocks are produced by a random walk on a pre-existing fracture system, resulting in the direct connection between the p-values and the fractal dimension of the pre-existing fracture system. This model implies that the fractal properties of aftershocks are constrained by the fractal structure of the pre-existing fracture system. Nanjo *et al.* (1998) derived the correlations among p, b and D_0 from analyzing the natural observable data of seismicity and active faults. Therefore Eq. 7 and the correlations in Nanjo *et al.* (1998) support the correctness of the implication from the model.

Mogi (1962, 1967) discussed the relationship between aftershock activity and the crustal heterogeneity caused by faulting. Yoshida and Mikami (1986) discussed the decrease of irregularities of stress or strength in the lithosphere with increasing time after the occurrence of the main shock, from the fractal analyses of the aftershock sequence of the 1984 Nagano-ken Seibu earthquake in Japan. Mikumo and Miyatake (1979) took a similar idea in a frictional fault model with nonuniform strength and presented a negative relationship between p and b by their simulation. The negative correlation between p and b in Nanjo *et al.* (1998) supports qualitatively the frictional fault model with nonuniform strength.

Enya (1901) hypothesized that main shock disturbs strain distribution and the aftershocks occur to decrease the heterogeneity of the strain distribution in the crust. In the SOC model of earthquakes, Ito and Matsuzaki (1990) took Enya's (1901) idea, and successfully derived scaling laws of earthquakes. However, these studies have not established the relationship between the fractal properties of aftershocks and pre-existing discontinuities in the lithosphere.

In general, internal structures and discontinuities in the lithosphere seem to influence earthquakes. Nagahama and Teisseyre (1998, 2000a,b) discussed the fractal properties of fracturing such as faulting or earthquakes in the lithosphere from the point of view of the continuum with microstructure (the micromorphic continuum). Nanjo *et al.* (1998) and this chapter establish that the structures of active fault systems essentially influence on the fractal properties of aftershocks. By comparing my results with previous studies, the crustal heterogeneity (Mogi, 1962, 1967), the irregularities of stress or strength in the lithosphere (Mikumo and Miyatake, 1979; Yoshida and Mikami, 1986) and the heterogeneity of strain distribution in the crust (Enya, 1901) may be regarded as the fractal structures of active fault systems.

Very often, special cluster patterns like Doughnut patterns of foreshocks have been pointed out (e.g., Mogi, 1985). Considering my results, I note that the cluster pattern of foreshocks may be related to the fractal structures of the active fault systems in which the earthquakes occur.

In conclusions, the relationship between D_2 and D_0 is expressed as $D_2 = (0.72 \pm 0.02)D_0 + (0.91 \pm 0.02)$. This correlation shows that the aftershock distribution tend to cluster more loosely with an increase in the fractal dimensions of the active faults in the aftershock region. If the fractal dimension of active fault system is the upper limit value of the fractal dimension of actual fracture geometries in rock, then clustering aftershocks show a completely random distribution. Therefore, I conclude that each cluster of the aftershocks shows the fractal properties under the constraints of the fractal structure of the active fault systems.

Chapter 4

Relationships between aftershock spatial distribution and earthquake fault lengths

"It costs only a dime."

4-1. Data of main shocks and aftershocks

In this chapter, I examine the relationships between the aftershock magnitude and the distance from the main shock to aftershocks. Moreover, the observed spatial distributions of aftershocks are investigated by associating with earthquake fault lengths. Then, I discuss earthquake fault length, and Båth's law (Richter, 1958).

I use data of the fourteen main shocks (Table 1) and their aftershocks analyzed in Chaps. 2 and 3. Aftershocks of magnitude larger than 2.0 are treated here. To evaluate distances between aftershocks and the main shocks, I estimate the shortest distances between the hypocenters.

4-2. Spatial distribution of aftershocks

Based on the relationship between the aftershock magnitudes and the hypocentral distances between the main shocks and aftershocks (Fig. 8), the spatial distributions of the upper limits of the aftershock magnitude are examined. The upper limits should be determined objectively. The aftershock with the largest magnitude in each 1km interval of hypocentral distance from the main shock is picked up. I apply the Stineman Function (Stineman, 1980) in the software 'Kaleida Graph' published by Synergy Software, to the data of the aftershocks picked up. This function will fit a smoothed curve to the data. I regard the smoothed curve fitted to the data picked up as the spatial distribution of the upper limit of the aftershock magnitude.

The curve shows that the upper limit decreases with fluctuation as the distance from the main-shock hypocenter increases, although it increases within adjacent distance to the main-shock hypocenter (Fig. 8). In the fluctuating decrease, I point out the one minimum, which is indicated by 'min.' in Fig. 8. The value of this minimum is one of the smallest values in minima of the curve, and then this minimum is the nearest to the main-shock hypocenter in the minima with the smallest values. Because of this minimum, the curve shows that the spatial distribution of the upper limit is bimodal, with a tendency of the upper limit to decrease as the distance from the main-shock hypocenter increases. For the six aftershock sequences of 1980's (Table 4), I observe the bimodal distributions. The other aftershock sequences show unclear bimodal distributions. It is due to the low quality of precisions to determine epicenters and depth.

In this study, I make further investigations into the observed spatial distributions. When the minimum pointed out above separates all aftershocks into two aftershock groups, I focus on the two aftershocks whose magnitude is the largest in each of the two aftershock groups. I_1, M_1, and T_1 show hypocentral distance from the main shock, magnitude, and time, respectively, of the largest aftershock in the aftershock group nearer to the main-shock hypocenter (Table 4). Similarly, I_2, M_2, and T_2 show hypocentral distance from the main shock, magnitude, and time, respectively, of the largest aftershock in the aftershock group further from the

Table 4 Main shocks and observed data. Magnitude (M_M) and rupture length (L (km)) of main shocks. Rupture length is not available for some events, indicated by '-'. I_1, M_1, and T_1: distance from main-shock hypocenter (km), magnitude, and elapsed time (day(s)), respectively, of the largest aftershock in the aftershock sequence nearer to main-shock hypocenter. I_2, M_2, and T_2: distance from main-shock hypocenter (km), magnitude, and elapsed time (day(s)), respectively, of the largest aftershock in the aftershock sequence further to main-shock hypocenter. #: the largest aftershock in each aftershock sequence.

Main shock	M_M	L	I_1	M_1	T_1	I_2	M_2	T_2
Boundary between Kanagawa and Yamanashi Prefectures	6.0	-	10.8	#5.2	191	17.2	4.0	141
Eastern Tottori Prefecture	6.2	5	6.8	#5.7	0	14.9	3.5	24
Near Unzen	5.7	-	5.7	#5.0	0	13.9	4.0	997
Nagano-ken Seibu earthquake	6.8	12	10.0	#6.2	1	22.9	4.9	540
Northern Nagano Prefecture	5.9	-	3.8	3.5	14	20.5	#3.6	615
Yamaguchi Prefecture	5.2	-	2.3	#3.6	3	6.3	3.2	791

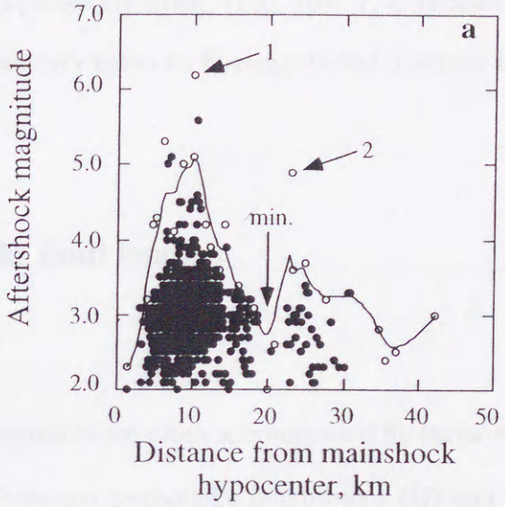

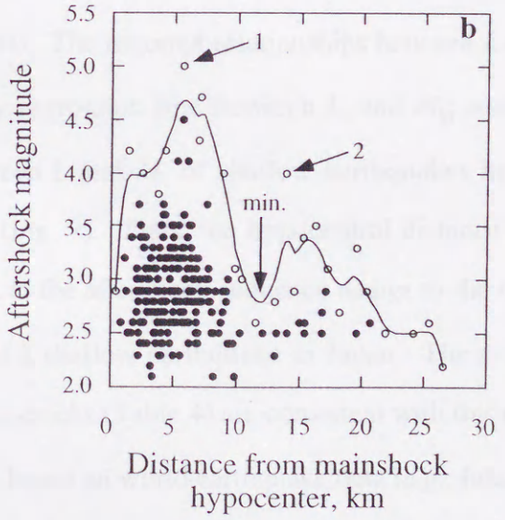

Fig. 8 Relationship between aftershock magnitude and the hypocentral distance between aftershock and main shock. (a) Nagano-ken Seibu earthquake. (b) Earthquake occurred near Unzen. Open and solid circles show aftershocks. Open circle is the largest aftershock in each 1km interval of hypocentral distance from the main shock. Solid curve shows the smooth curve fitted to the open circles. The value of the minimum, represented by 'min.', is one of the smallest values in minima of the curve and then this minimum is the nearest to the main-shock hypocenter in the minima with the smallest values. The aftershocks indicated by '1' and by '2' are the largest aftershocks in the aftershock sequences nearer to and further to main-shock hypocenter, respectively.

main-shock hypocenter (Table 4). I_1 and I_2 correlate positively to the main-shock magnitude (M_M) (Fig. 9). M_1 is larger than M_2, except for the earthquake occurred in the northern Nagano prefecture (Table 4). Since two data of $M_1 < 5.0$ apparently underlie a general relationship between M_1 and M_M, the least upper bound of M_1 correlates positively to M_M (Fig. 10). M_2 correlates positively to M_M (Fig. 10). T_1 is smaller than T_2, except for the earthquake occurred at the boundary between Kanagawa and Yamanashi Prefectures (Table 2).

4-3. Earthquake fault lengths

Some earthquakes are often accompanied by surface breaks. Previous studies reported the relationships between earthquake magnitudes (M) and the lengths of surface breaks (L), based on earthquake data (e.g., Iida, 1965; Matsuda, 1977; Bonilla *et al.*, 1984; Wells and Coppersmith, 1994). The reported relationships between L and M vary from one investigator to the other. My regression line between I_1 and M_M statistically corresponds only to the relationship between L and M, of shallow earthquakes in Japan, $M = 1.7\log L$ (km) + 4.8 (Matsuda, 1977) (Fig. 9). Thus, the hypocentral distance between the main shock and the largest aftershock in the aftershock sequence nearer to the main-shock hypocenter is equal to the fault length of a shallow earthquake in Japan. The available lengths (L) of the surface breaks of the main shocks (Table 4) are consistent with this result. However, the relationships between L and M, based on world earthquake data (e.g., Iida, 1965; Bonilla *et al.*, 1984; Wells and Coppersmith, 1994), do not correspond to my regression line between I_1 and M_M.

Using data of world earthquakes, several researchers found the upper limits of earthquake fault lengths for each M, and these limits are called maximum earthquake fault length (L_{MAX}) (Otsuka, 1964; Iida, 1965; Yonekura, 1972). L_{MAX} increases with increasing M, $M = 2.0\log L_{MAX}$ (km) + 3.6 (Otsuka, 1964), $M = 2.0\log L_{MAX}$ (km) + 3.5 (Iida, 1965) and $M = 2.0\log L_{MAX}$ (km) + 3.7 (Yonekura, 1972). These relationships are close each other (Fig. 9). My regression line

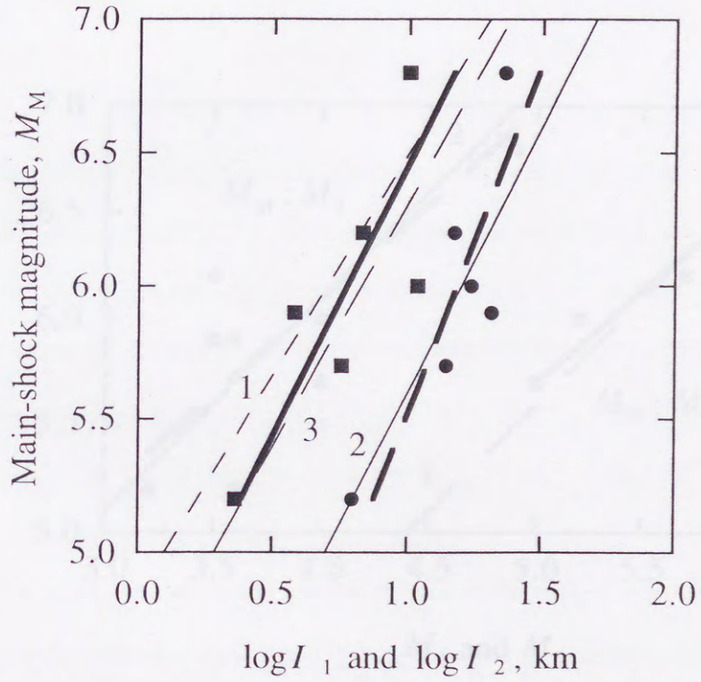

Fig. 9 Relationship between I_1 (square) and M_M and relationship between I_2 (circle) and M_M. Thick solid line and thick long-dashed line represent least-square regressions; $M_M = (2.04 \pm 0.47)\log I_1 + (4.41 \pm 0.36)$ and $M_M = (2.64 \pm 0.48)\log I_2 + (2.88 \pm 0.56)$, respectively. Thin long-dashed line (1) shows Matsuda (1977)'s relationship between L and M. Because the relationships between L_{MAX} and M (Otsuka, 1964; Iida, 1965; Yonekura, 1972) are close each other, we show only Otsuka (1964)'s relationship (2: thin-solid line). Thin short-dashed line (3) indicates the relationship between D_L and M_M (Hosono and Yoshida, 1991).

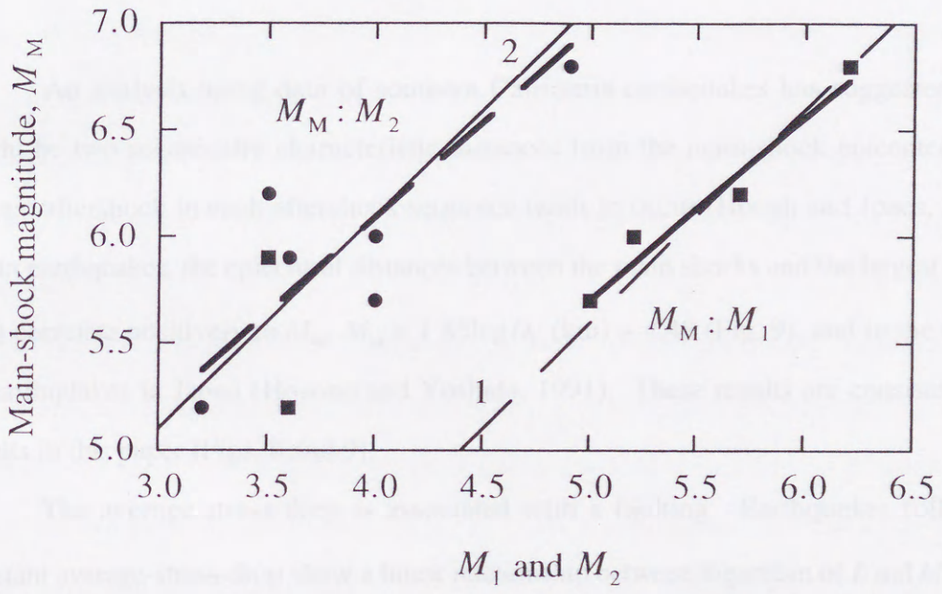

Fig. 10 Relationship between M_1 (square) and M_M and relationship between M_2 (circle) and M_M. The least-square regression between M_1 and M_M for data of $M_1 \geq 5.0$ is expressed as $M_M = (0.86 \pm 0.02)M_1 + (1.40 \pm 0.11)$ (thick-solid line). The least-square regression between M_2 and M_M is $M_M = (0.90 \pm 0.19)M_2 + (2.49 \pm 0.74)$ (thick dashed line). Thin-dashed line and thin-solid line represent $M_M - M_1 = 0.6$ (1) and $M_M - M_2 = 2.1$ (2), respectively.

between I_2 and M_M statistically corresponds to the relationships between L_{MAX} and M (Fig. 9). Thus, the hypocentral distance between the main shock and the largest aftershock in the aftershock sequence further to the main-shock hypocenter is equal to the maximum earthquake fault length. It is a future research to study the tectonic implications of the occurrence of this largest aftershock, because the region away from the main-shock hypocenter by the distance of I_2 might have played some essential role in the preparatory process of generating earthquake.

4-4. Discussions

An analysis using data of southern California earthquakes has suggested that there might be two seismically characteristic distances from the main-shock epicenter where the largest aftershock in each aftershock sequence tends to occur (Hough and Jones, 1997). For Japan earthquakes, the epicentral distances between the main shocks and the largest aftershocks (D_L) correlate positively to M_M, $M_M = 1.85\log D_L$ (km) + 4.48 (Fig. 9), and to the fault length of earthquakes in Japan (Hosono and Yoshida, 1991). These results are consistent with the results in this paper (Figs. 8 and 9).

The average-stress-drop is associated with a faulting. Earthquakes followed by a constant average-stress-drop show a linear relationship between logarithm of L and M (Kanamori and Allen, 1986) with slope 1.7 - 2.0 (Tsuboi, 1956; Nagahama, 1994b). The value of this slope is similar to that of my regression between I_1 and M_M and to that of Matsuda (1977)'s relationship between L and M (Fig. 9). This similarity deduces that average-stress-drop is a constant for earthquakes in Japan inland.

For the available two cases having the information about the faulting process and the geometry of the main-shock rupture (Table 4), I investigate the relationship between the geometry of earthquake fault of the main shock and the epicentral distribution of aftershocks. Both main shocks have mechanism solution of strike-slip type (Sato *et al.*, 1989). For the

Nagano-ken Seibu earthquake, the largest aftershock in the aftershock group nearer to the main-shock hypocenter occurs at the edge of the main-shock rupture (Fig. 11). However, considering the earthquake occurred at the eastern Tottori prefecture (Fig. 12), the occurrence of the aftershock appears to be not always related with the geometry of the main shock. Note that the selection of the main shocks in this study is irrelevant to the style of faulting. This is due to that the relationships between L and M are not different for the style of faulting (Wells and Coppersmith, 1994). However, past studies (e.g., Kanamori and Anderson, 1975; Bonilla *et al.*, 1984) have demonstrated that the faulting style is significant for correlation between L and M. Thus, for example, the analyses only for shallow earthquakes having mechanism solutions of strike-slip type might be required future studies.

Båth's law (Richter, 1958) is expressed as $M_M = M_L + q$, where M_L is magnitude of the largest aftershock and q is constant of 0.1 to 3 with an average value of 1.2. If $q = 1.2$ then the energy released by the largest aftershock is equal to 2 % of that by the main shock. My regression between M_M and M_1 is similar to Båth's law of $q = 0.6$ (Fig. 10). Moreover, my regression between M_M and M_2 is similar to Båth's law of $q = 2.1$ (Fig. 10). Thus, the two magnitude correlations between the main shock and the largest aftershocks in the two aftershock sequences are similar each other, like Båth's law. q may be an important parameter because q must depend on the ratio of energy cascades associated with material properties. In this paper, my analyses are restricted to the six aftershock sequences. This restriction may depend on the errors of the hypocentral locations, because the earthquakes are detected with the highest precision in the file and their detection thresholds do not vary from one main shock to the other. To examine much more cases with small errors might require further researches.

In conclusions, the spatial distributions of the upper limit of the aftershock magnitudes were examined as a function of the hypocentral distances between the main shocks and aftershocks. For aftershock sequences follow the six main shocks of focal depth shallower than 20 km with magnitude more than 5.0 from 1983 to 1987 in Japan, I found that the spatial distributions are bimodal, with a tendency of the upper limit to decrease as the distance from the main-shock hypocenter increases. To make further investigations, all aftershock data

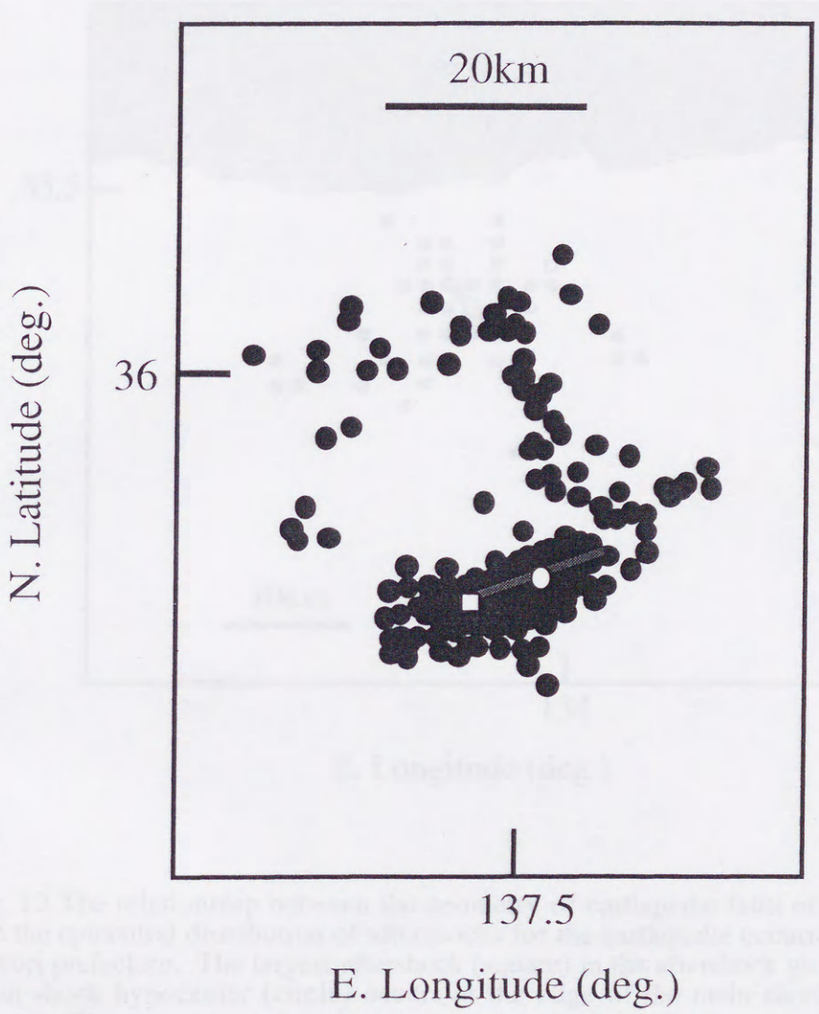

Fig. 11 The relationship between the geometry of earthquake fault of the main shock and the epicentral distribution of aftershocks for the Nagano-ken Seibu earthquake. The largest aftershock (square) in the aftershock group nearer to the main-shock hypocenter (circle) occurs at the edge of the main-shock rupture (solid curve). The main shock has the mechanism solution of strike-slip type (Sato *et al.*, 1989).

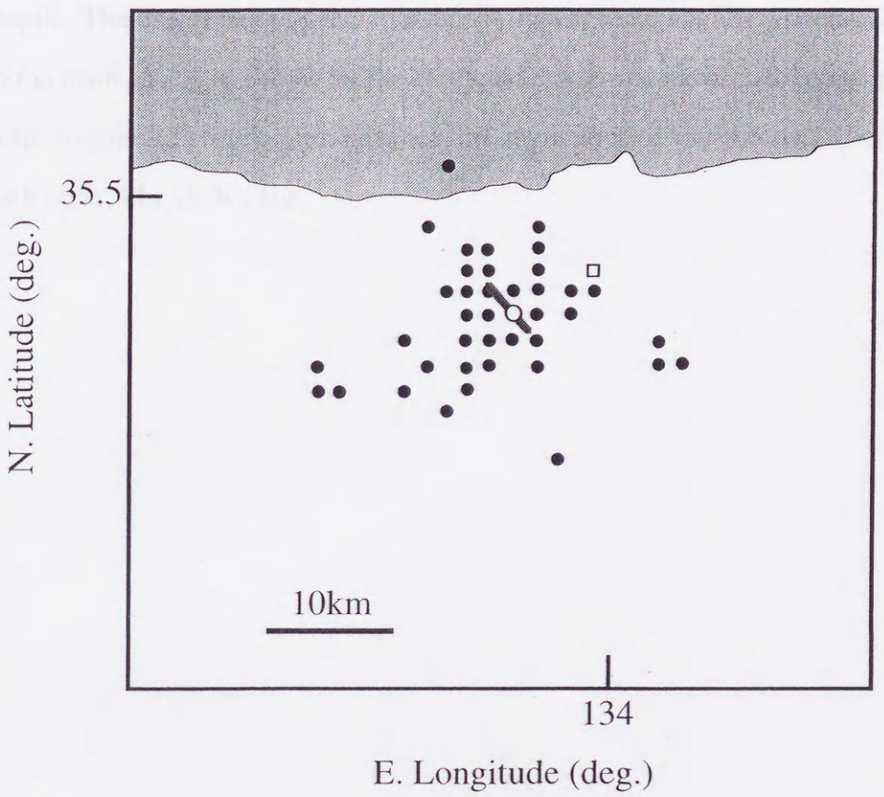

Fig. 12 The relationship between the geometry of earthquake fault of the main shock and the epicentral distribution of aftershocks for the earthquake occurred at the eastern Tottori prefecture. The largest aftershock (square) in the aftershock group nearer to the main-shock hypocenter (circle) occurs at the edge of the main-shock rupture (solid curve). The main shock has the mechanism solution of strike-slip type (Sato *et al.*, 1989).

were separated into the two aftershock sequences constituting the bimodal distribution. Then, I focused on the two aftershocks, which are the largest in the two aftershock groups. It was found that the hypocentral distances between the main shocks and the two aftershocks are equal to the fault length of shallow earthquakes in Japan and to the maximum earthquake fault length. The occurrences of the aftershocks appear to be not always related with the geometry of the main shock, as shown by the earthquake occurred in eastern Tottori prefecture. Finally, both magnitude correlations between the main shocks and the two aftershocks are similar each other, like Båth's law.

Chapter 5

Symmetropy in rock fracture experiment and self-organized criticality

"Fearful Symmetry: Is God a Geometer?"

by I. Stewart and M. Golubitsky, 1992.

5-1. Symmetropy

According to Yodogawa (1982), I introduce 'symmetropy'. He utilized that the two-dimensional discrete Walsh functions are divided into the four types of symmetry: vertical symmetry, horizontal symmetry, centrosymmetry, and double symmetry (Fig. 13). Here Walsh function (Walsh, 1999) is a closed set of normal orthogonal functions. And he quantified these four types of the symmetry in a pattern. The symmetropy is based on the quantities of the symmetries

Patterns used in this paper are restricted to rectangular matrix, each consisting of $G \times H$ rectangular cells, where $G = 2^y$ and $H = 2^z$ (y and z are positive integers). The two-dimensional discrete Walsh transform of a pattern is given by

$$a_{g,h} = \frac{1}{GH} \sum_{d=0}^{H-1} \sum_{e=0}^{G-1} x_{d,e} W_{g,h}(d, e), \tag{8}$$

$g = 0, 1, 2, \ldots, G - 1$ and $h = 0, 1, 2, \ldots, H - 1$,

where $x_{d,e}$ is the value of gray level of a pattern in the e th row cell in the d th column, $W_{g,h}(d, e)$ is the value (1 or -1) of the (g, h) th order of the two-dimensional discrete Walsh function in the e th row cell in the d th column (Fig. 13), and $a_{g,h}$ is the two-dimensional Walsh spectrum. If there are just two gray levels: 'black' and 'white', I usually represent $x_{d,e}$ by 1 and 0.

Symmetric component Q_k ($k = 1, 2, 3, 4$) quantifying the four types of symmetry is given by

$$Q_k = \sum_{g,h} (a_{g,h})^2 / K, \tag{9}$$

where $K = \sum_{h=0}^{H-1} \sum_{g=0}^{G-1} (a_{g,h})^2 - (a_{0,0})^2$ and $\sum_{k=1}^{4} Q_k = 1$. Vertically symmetric component Q_1 is given when g = even and h = odd. Horizontally symmetric one Q_2 is given when g = odd and h = even. Centrosymmetric one Q_3 is given when g = odd and h = odd. Doubly symmetric one Q_4 is given when g = even and h = even. The sum is taken over all ordered pairs (g, h) for $0 \le g \le G - 1$ and $0 \le h \le H - 1$ where $a_{0,0}$ is excepted.

When one applies the entropy function in information theory to Q_k ($k = 1, 2, 3, 4$), the symmetropy S is given by

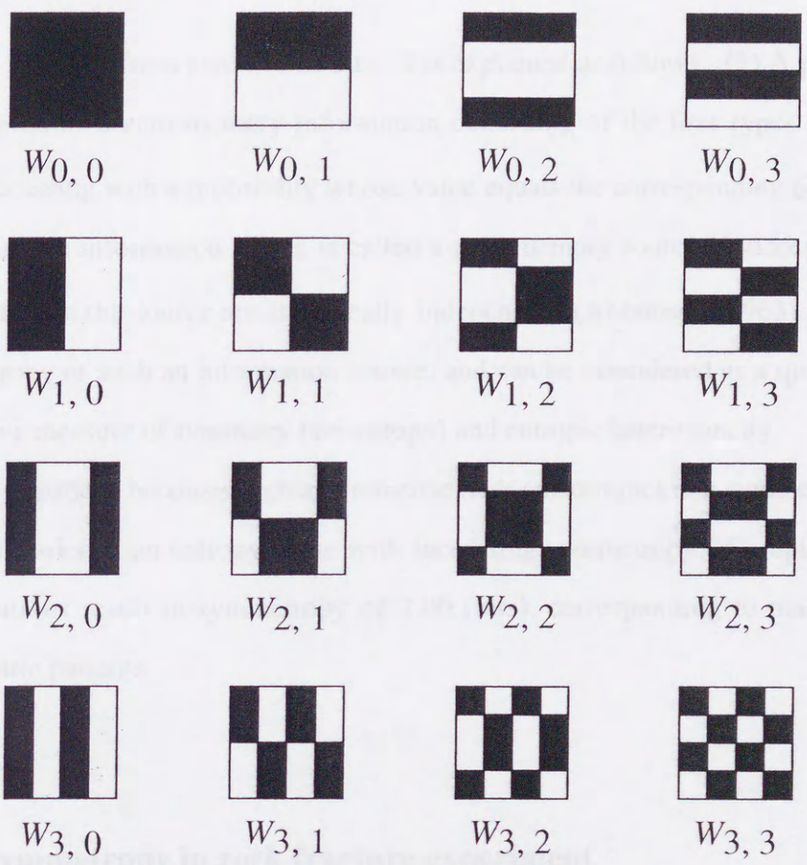

Fig. 13 The first 16 of the two-dimensional discrete Walsh functions $W_{g,h}$ ($G = H = 4$). Black and white represent 1 and −1, respectively. $W_{g,h}$ is vertically symmetric when g = even and h = odd, is horizontally symmetric when g = odd and h = even, is centrosymmetric when g = odd and h = odd, and is doubly symmetric when g = even and h = even, where $W_{0,0}$ is excepted.

$$S = -\sum_{k=1}^{4} Q_k \log_2 Q_k. \qquad (10)$$

S ranges from zero to two bits. S is explained as follows: (1) A pattern can be considered as a zero-memory information consisting of the four types of symmetry, each occurring with a probability whose value equals the corresponding Q_k (k = 1, 2, 3, 4). Here, an information source is called a zero-memory source if successive symbols emitted from the source are statistically independent (Abramson, 1963). (2) S means the entropy of such an information source, and can be considered as a quantitative and objective measure of symmetry (anisotropy) and entropic heterogeneity.

A pattern becomes higher symmetric (less anisotropic) in a symmetry sense and more disorder in an entropy sense with increasing symmetropy. Completely random distributions result in symmetropy of 2.00 (bits), corresponding to macroscopically symmetric patterns.

5-2. Symmetropy in rock fracture experiment

5-2-1. Fracture experiment

In this paper, I analyze the 9 spatial distributions of AE events generated by microfracturings within rock, published in Hirata *et al.* (1987). Here, I briefly review the rock fracture experiment and the results of Hirata *et al.* (1987).

A constant stress fracture experiment of Oshima granite was carried out at the confining pressure of 40 MPa. The rock specimen is a cylinder 50 mm in diameter and

Table 5 Estimated values of Q_k (k = 1, 2, 3, 4) and S (bits).

	left			right			top		
	primary	secondary	tertiary	primary	secondary	tertiary	primary	secondary	tertiary
Q_1	0.17	0.17	0.11	0.18	0.14	0.12	0.19	0.20	0.09
Q_2	0.16	0.16	0.09	0.15	0.14	0.09	0.19	0.21	0.21
Q_3	0.14	0.14	0.11	0.15	0.15	0.09	0.22	0.18	0.08
Q_4	0.53	0.53	0.69	0.52	0.57	0.70	0.40	0.41	0.62
S	1.74	1.74	1.38	1.76	1.67	1.35	1.92	1.91	1.50

100 mm long (Fig. 14). The creep is divided into three stages: primary creep, secondary creep, and tertiary creep. The spatial distributions of 353, 273, and 1438 events of AE detected during the primary, secondary, and tertiary creep, respectively, showed fractal properties. The fractal dimensions decreased from 2.75 via 2.66 to 2.25 as creep progressed. Hirata *et al.* (1987) showed orthographic projections at each of the three stages (Fig. 14). AE events distributing within the three-dimensional rock are projected on 3 planes: one plane has a normal vector which is perpendicular to circular (top) side of the cylinder; and each of the two others has a normal vector which is perpendicular to straight parallel sides of the cylinder, and the planes are situated on the left of and on the right of the cylinder.

5-2-2. Procedure and results

I regard the AE events as circles with finite diameter. The circles are equal to circles to draw AE events in Hirata *et al.* (1987). I analyze the spatial distributions of AE plotted within rock. $(G, H) = (64, 32)$ for the spatial distributions projected on the planes on the left of and on the right of the specimen (Fig. 14), and $(G, H) = (32, 32)$ for the spatial distributions projected on the plane on the top of the specimen. If one find a part of or whole of one or more of circles in a cell of (d, e), then $x_{d, e} = 1$, otherwise $x_{d, e} = 0$ (Fig. 14). According to Yodogawa (1982), I estimate Q_k ($k = 1, 2, 3, 4$) and S for the 9 spatial distributions of AE.

Table 5 shows the estimated values of Q_k ($k = 1, 2, 3, 4$) and S (bits). $0.09 \leq Q_1 \leq 0.20$, $0.09 \leq Q_2 \leq 0.21$, $0.08 \leq Q_3 \leq 0.22$, $0.40 \leq Q_4 \leq 0.70$, and $1.35 \leq S \leq 1.92$. For each of the 9 projected spatial distributions of AE, Q_4 is larger than Q_k ($k = 1, 2, 3$). Moreover, the ranges of Q_k ($k = 1, 2, 3$) almost equal each other and the upper limit of

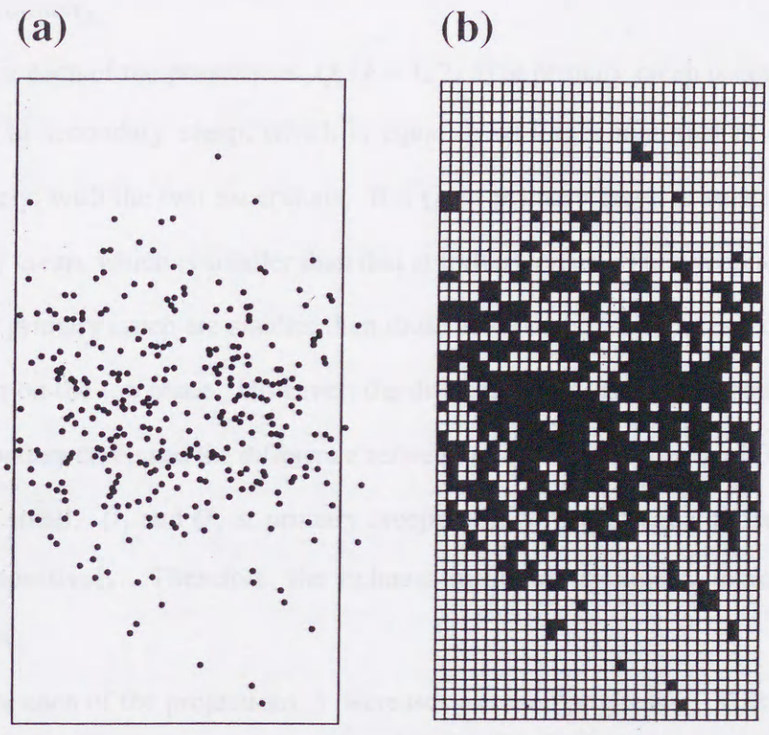

Fig. 14 An example of the spatial distribution of AE events occurring in rock specimen. (a) 273 events occurring at primary creep are projected orthographically on the plane of a normal vector, which is perpendicular to straight parallel sides of the cylinder rock specimen (modified from Hirata *et al.*, 1987). The plane is situated on the left of the rock specimen. (b) 64 × 32 cells cover rock specimen. Black cells contain a part of or whole of one or more of AE events. 1 and 0 are given to black and white cells, respectively. The estimated values of Q_k (k = 1, 2, 3, 4) and S are 0.17, 0.16, 0.14, 0.53, and 1.74 (bits), respectively.

Q_k (k = 1, 2, 3) is 0.22, while the lower limit of Q_4 is 0.40. That is, Q_4 is clearly larger than Q_k (k = 1, 2, 3). Therefore, the spatial distributions of AE are clearly rich in double symmetry.

For each of the projections, Q_k (k = 1, 2, 3) at primary creep is equal to or larger than that at secondary creep, which is equal to or larger than that at tertiary creep, respectively, with the two exceptions. But Q_4 at primary creep is smaller than that at secondary creep, which is smaller than that at tertiary creep. The exceptions are that Q_1 and Q_2 at primary creep are smaller than those at secondary creep, respectively, for the projection on the top plane. However, the difference between Q_1 at primary creep and Q_1 at secondary creep and the difference between Q_2 at primary creep and Q_2 at secondary creep are small. Q_1 and Q_2 at primary creep are regarded to equal those at secondary creep, respectively. Therefore, the richness in double symmetry increases as creep progresses.

For each of the projections, S decreases as creep progresses. This decrease of S comes from the increase of the richness in double symmetry.

Using symmetropy, I established the method to measure quantitatively the anisotropy and entropic heterogeneity of the spatial distributions of microfractures, and moreover to detect their changes with progressing the creep. Because earthquakes are regarded as the SOC phenomena (e.g., Bak and Tang, 1989; Ito and Matsuzaki, 1990), I estimate also the symmetropy of the spatial patterns of earthquakes (fractures) in the SOC model.

5-3. Symmetropy in self-organized criticality

I perform the sand-pile cellular-automaton model (e.g., Bak, 1996; Turcotte,

1999) of a square grid of 64 × 64 square cells in two dimensions (Fig. 15) according to the code written by Jensen (1998). This is a SOC model for the occurrences of earthquakes or fractures. An avalanche corresponds to one earthquake or one fracturing. The system starts from an initial condition where the number of particles for all cells is zero. It evolves through sub-critical states and reaches the critical steady state at about 9.0×10^3 time steps (Fig. 15). I estimate the symmetropies S_1 of the spatial patterns of avalanches occurring in various time spans (Fig. 16a-d). The symmetropies S_1 are the constant close to two bits irrespective of time spans during sub-critical states (Fig. 17). This result shows that the resultant patterns are completely disorder and macroscopically symmetric. During the critical steady states, the symmetropies S_1 range from 1.52 to 1.94 bits (Fig. 17). This result shows the emergence of variety of order in the resultant patterns. Moreover, I quantitatively detect the anisotropy of spatial patterns of avalanches. Additionally, I estimate the symmetropies S_2 for the spatial patterns of the active cells, each at which the first redistribution in an avalanche occurs, in various time spans (Fig. 16ef). The symmetropies S_2 are exactly 2.00 bits irrespective of the time spans and the system's states (Fig. 17). This result indicates that the decrease of S_1 from two bits is due directly to avalanche dynamics of the critical states, not dependent on the arrangement of the first redistribution cells.

5-4. Discussions

I examined the symmetropy of the spatial distributions of AE events generated in the laboratory experiment carried out by Hirata *et al.* (1987). Moreover, I apply the symmetropy to the spatial patterns of earthquakes in the SOC model for fracturing (e.g., Bak and Tang, 1989; Bak, 1996; Jensen, 1998; Turcotte, 1999). Using symmetropy

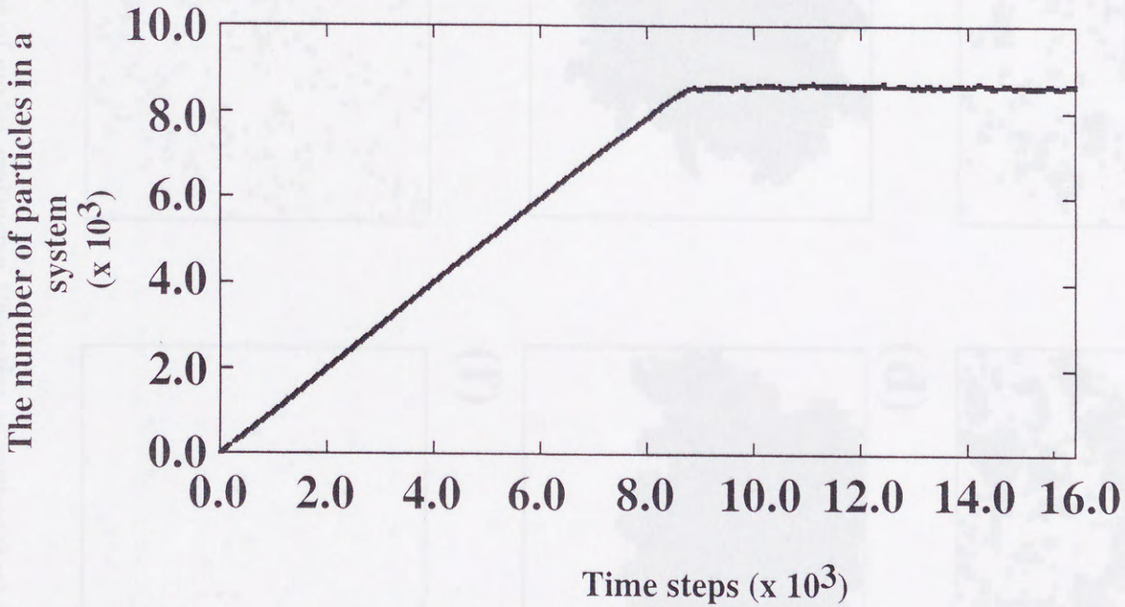

Fig. 15 The number of particles in a system of 64 × 64 square grid as a function of time steps. The system transforms from sub-critical state to critical one at about 9×10^3 step.

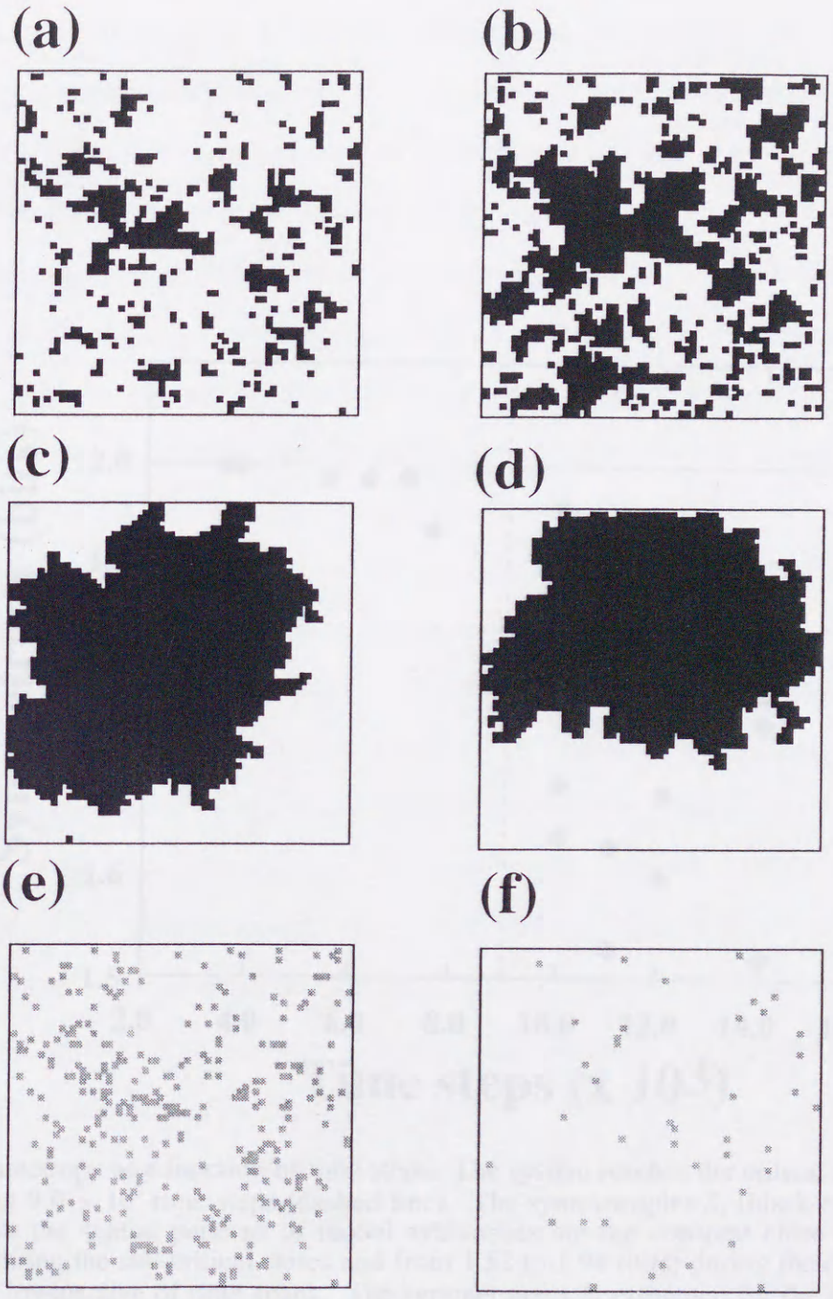

Fig. 16 Spatial patterns of model avalanches (fractures or earthquakes) and of the cells from which avalanches start in a 64 × 64 square grid. Black cells take participate in avalanches occurring from 4501 to 6500 time steps (a), from 5001 to 7500 time steps (b), from 10001 to 10020 time steps (c) and from 14001 to 14010 time steps (d). a and b are in the sub-critical states and, c and d are in the critical steady states. Each of the grey cells is the cell at which the first redistribution in an avalanche occurs, from 4501 to 6500 time steps during the sub-critical states (e) and from 11001 to 11100 time steps during the critical steady states (f). The symmetropies of a, b, c, d, e and f are 1.99, 1.99, 1,96, 1.52, 2.00 and 2.00 (bits), respectively. The symmetropies in this paper are estimated for the spatial patterns of avalanches and the first redistribution cells during various time spans. Colored cells get 1 and others get 0 for symmetry analyses.

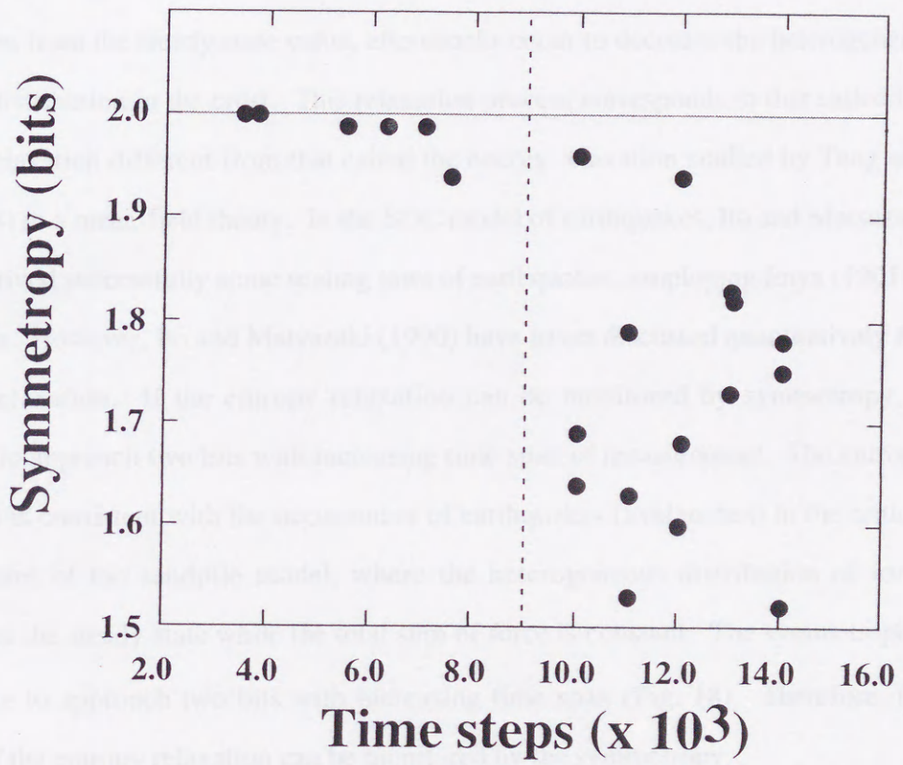

Fig. 17 Symmetropy as a function of time steps. The system reaches the critical steady state at about 9.0×10^3 time steps (dashed line). The symmetropies S_1 (black circles) estimated for the spatial patterns of model avalanches are the constant close to the maximum during the sub-critical states and from 1.52 to 1.94 (bits) during the critical steady state irrespective of time spans. The symmetropies S_2 estimated for the spatial patterns of the cells from which avalanches start, are exactly 2.00 (bits) irrespective of time spans and the system's state, indicated by a grey line.

allows us to establish the method to measure quantitatively the anisotropy and entropic heterogeneity of the spatial distributions of (micro)fractures in the rock fracture experiment and in the SOC model of earthquakes. This establishment provides a new measure to evaluate collective properties of earthquakes and active faults.

Aftershock is a kind of relaxation phenomena. Enya (1901) submitted the models concerning the origin of aftershocks that because the main shock disturbs strain distribution from the steady state value, aftershocks occur to decrease the heterogeneity of strain distribution in the crust. This relaxation process corresponds to that called the entropy relaxation different from that called the energy relaxation studied by Tang and Bak (1988) in a mean-field theory. In the SOC model of earthquakes, Ito and Matsuzaki (1990) derived successfully some scaling laws of earthquakes, employing Enya (1901)'s hypothesis. However, Ito and Matsuzaki (1990) have never discussed quantitatively the entropy relaxation. If the entropy relaxation can be monitored by symmetropy, it increases to approach two bits with increasing time span of measurement. The entropy relaxation is consistent with the occurrences of earthquakes (avalanches) in the critical steady states of the sandpile model, where the heterogeneous distribution of force approaches the steady state while the total sum of force is constant. The symmetropies S_1 increase to approach two bits with increasing time span (Fig. 18). Therefore, the process of the entropy relaxation can be monitored by the symmetropy.

The curie symmetry principle (CSP) does not allow us to infer the symmetriic cause for interpreting the lower symmetric (anisotropic) pattern in the resultant effect in a physical process (e.g., Curie, 1894; Jaeger, 1920; Rosen, 1995). Previous results (Nicolis and Prigogine, 1977; Sattinger, 1978; Bouligand, 1985; Stewart and Golubitsky, 1992; Nakamura and Nagahama, 2000) show, however, that one cannot invoke the CSP undoubtedly for all fields. The symmetry aspect of the causality relation between the symmetry of the cause and the resultant effect in the SOC system seems to show symmetry breaking. In a future research, I will discuss the symmetry breaking in the SOC system.

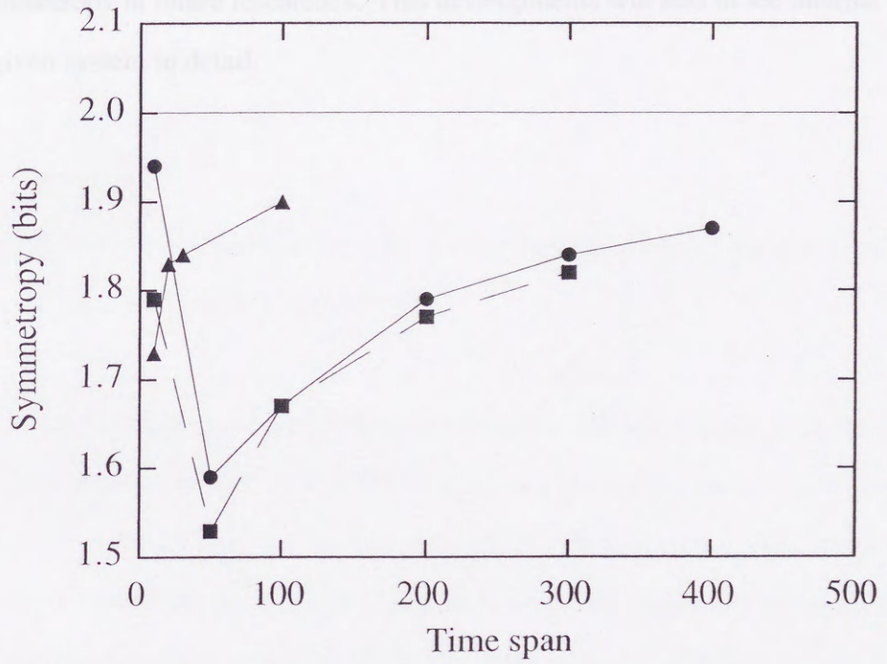

Fig. 18 Symmetropy as a function of time span from 10001 step (circle), from 11001 step (square) and from 12001 step (triangle).

'Symmetropy' that can measure symmetry and entropy of objects, meets a claim that there is no perfect symmetry in nature. In the present work, I applied the symmetropy to the spatial distributions of the microfracturing events in rock and the resultant patterns of the model avalanches in the SOC model. This new measure 'symmetropy' is expected to be a powerful tool to measure symmetry and entropy for many fields of sciences, particularly for the study of complex systems. Considering the results of Chaps. 2 and 3 and 5 (this chapter), one needs to develop the scale-invariant representation of spectra of symmetropy in future researches. This developments will lead to see internal structure of a given system in detail.

Chapter 6

Conclusions

In this paper, I studied the collective properties of earthquakes and active faults. The results are summarized as follows:

(1) Aftershock sequences following earthquakes (main shocks) in Japan and active fault systems within their aftershock regions satisfy the modified Omori formula of aftershocks and the Gutenberg-Richter relation. Moreover, they show the fractal properties for the spatial distributions of epicenters and active faults. These are taken as circumstantial evidence of earthquakes of SOC phenomena.

(2) The fractal dimensions of the epicentral distributions of aftershocks correlate positively with those of the pre-existing active fault systems in the aftershock regions. The correlation shows that the aftershock distributions become less clustered with increasing the fractal dimensions of the active fault system. That is, the clusters of the aftershocks are constrained under the fractal properties of the pre-existing active fault systems.

(3) If the fractal dimension of active fault system is the upper limit value of the fractal dimension of actual fracture geometries of rocks, then the clustering aftershocks show a completely random distribution.

(4) The spatial distributions of the upper limit of aftershock magnitudes were examined as a function of the hypocentral distances between the main shocks and aftershocks. The spatial distributions are bimodal, with a tendency of the upper limit to decrease as the distance from the main-shock hypocenter increases. I focused on the largest aftershocks in each of the two aftershock groups constituting the bimodal distribution. The distances of the two largest aftershocks from the main-shock hypocenter are equal to the fault lengths of shallow earthquakes in Japan and to the maximum earthquake fault lengths. The occurrence of the aftershock appears to be not always related with the geometry of the main shock, as shown by the earthquake occurred in eastern Tottori prefecture. Moreover, both magnitude correlations between the main shock and the two aftershocks are similar each other, like Båth's law.

(5) I introduced the concept of the symmetropy. Using symmetropy allows us to establish the method to measure quantitatively the anisotropy and entropic heterogeneity of the spatial distributions of (micro)fractures in the rock fracture experiment and in the SOC model of earthquakes.

(6) The symmetropies S_1 increase to approach two bits with increasing time span of measurement in the SOC state. Considering the entropy relaxation is consistence of the entropy relaxation with the occurrences of earthquakes (avalanches) in the SOC state, therefore, the process of the entropy relaxation can be monitored quantitatively by the symmetropy.

Finally I studied the earthquakes and the active faults as an ensemble, analyzing the observable data of the natural earthquakes and the active fault systems in the crust and the microfracturing events in rock fracture experiment as well as the avalanche dynamics simulated in the SOC model. My results demonstrated that earthquakes and active faults show collective properties, that cannot be understood by studying individual

earthquakes.

Acknowledgments

I wish to express my sincere thanks to Hiroyuki Nagahama of the Institute of Geology and Paleontology, Graduate School of Science, Tohoku University, for his critical reading of the manuscript, encouragement and guidance throughout the course of the present study. This thesis is made under his supervision. I also thank to Kenshiro Otsuki of the Institute of Geology and Paleontology, Graduate School of Science, Tohoku University, for his encouragement and guidance throughout the course of the present study.

The present author thanks M. Satomura of Institute of Biology and Geosciences, Faculty of Science, Shizuoka University, Y. Ogata of the Institute of Statistical Mathematics, T. Engelder of the Department of Geosciences, the Pennsylvania State University, K. Ito of the Department of Complex systems, The Future University-Hakodate, I. G. Main of Department of Geology and Geophysics, Grant Institute, University of Edinburgh, M. Kupkova of the Institute of Experimental Physics, Slovak Academy of Sciences, Y. Kagan, Department of Earth and Space Science, University of California, C. Kisslinger, Cooperative Institute for Research in Environmental Sciences and Department of Geological Sciences, University of

Colorado, and anonymous reviewers of Nanjo *et al.* (1998) and Nanjo and Nagahama (2000), for their valuable discussions and comments and for revising the English style of the earlier version manuscript on Chaps. 2 and 3.

I express my gratitude to K. Suyehiro of the Japan Marine Science and Technology Center (JAMSTEC), M. Ehiro of the Institute of Geology and Paleontology, Graduate School of Science, Tohoku University and N. Nakamura of the Tohoku University Museum, for their valuable comments on Chap. 4. Moreover, I am grateful to T. Dilov of the Institute of Geology and Paleontology, Graduate School of Science, Tohoku University, for improving English style of an earlier version of Chap. 4.

The author is grateful to E. Yodogawa of the Department of Computer Science and Communication Engineering, Kogakuin University, R. Takaki of the Institute of Mechanical System Engineering, Faculty of Engineering, Tokyo University of Agriculture and Technology, D. Nagy, Institute of Applied Physics, Faculty of Engineering, University of Tsukuba, K. Yamasaki of Department of Earth and Planetary Sciences, Faculty of Science, Kobe University, and an anonymous reviewer of Nanjo *et al.* (2000), for valuable and helpful comments and discussions on Chap. 5. Thanks are due to H. Hayashi and T. Chiba of the Institute of Geology and Paleontology, Graduate School of Science, Tohoku University, for helping computer programming.

I thank to Y. Ishikawa of Meteorological Research Institute, and the Disaster Prevention Research Institute (DPRI) of Kyoto University, for permission to use the file 'SEIS-PC' and the earthquake catalogue, respectively. My gratitude is extended to Research Fellowships of Japan Society for the Promotion of Science for Young

Scientists, for financial support.

I gratefully acknowledge my colleagues T. Asaki, N. Taniguchi, H. Hayashi, N. Sagawa, A. Ando, Y. Sekido, A. Takeuchi, A. Higano, H. Kanoh, D. Tsvetan, T. Chiba, A. Kuroyanagi, J. Nemoto, and A. Kohata, of the Institute of Geology and Paleontology, Graduate School of Science, Tohoku University, for valuable discussions and technical preparations of this paper.

Finally, my father Katsuhiko Nanjo, my mother Hisae Nanjo, and my younger brother Tatsuo Nanjo helped me any time. The author thanks Miyagi-ken Sports Center for offering me the place to take exercise.

References

Abramson, N., 1963. Information Theory and Coding. McGraw-Hill, New York.

Aki, K., 1981. Probabilistic synthesis of precursory phenomena. In: Simpson, D.W., Richards, P.G. (Eds.), Earthquake Prediction: An International Review. Maurice Ewing 4, Am. Geophys. Union, Washington, D.C., pp. 566-574.

Aviles, C.A., Scholz, C.H., Boatwright, J., 1987. Fractal analysis applied to characteristic segments of the San Andreas fault. J. Geophys. Res. 92, 331-344.

Bak, P., 1996. How Nature Works: The Science of Self-organized Criticality. Copernicus, New York.

Bak, P., Chen, K., Creutz, M., 1989. Self-organized criticality in the 'Game of Life'. Nature 342, 780-782.

Bak, P., Tang, C., 1989. Earthquakes as a self-organized critical phenomenon. J. Geophys. Res. 94, 15635-15637.

Bak, P., Tang, C., Wiesenfeld, K., 1988. Self-organized criticality. Phys. Rev. A 38, 364-374.

Barton, C.C., Larsen, E., 1985. Fractal geometry of two-dimensional fracture networks at Yucca Mountain, southwestern Nevada. In: Stephansson, O. (Ed.), Fundamentals

of Rock Joints. Proc. Int. Symp. Fundamentals of Rock Joints, Lulea, Sweden, pp. 77-84.

Bonilla, M.G., Mark, R.K., Lienkaemper, J.J., 1984. Statistical relations among earthquake magnitude, surface rupture length, and surface fault displacement. Bull. Seismol. Soc. Am. 74, 2379-2411.

Bouligand, Y., 1985. Symmetry principle and morphogehetic games. In: Demongeot, J., Goles, E., Tchuente, M. (Eds.), Dynamical Systems and Cellular Automata. Acad. Press Inc., London, pp. 75-86.

Brown, S.R., Scholz, C.H., 1985. Broad bandwidth study of the topography of natural rock surfaces. J. Geophys. Res. 90, 12575-12582.

Caillois, R., 1973. La Dissymetrie. Gallimard, Paris.

Caputo, M., 1976. Model and observed seismicity represented in a two-dimensional space. Ann. Geophys. 4, 277-288.

Curie, P., 1894. Sur la symerie dans les phenomenes physiques, symerie d'un champ electrique et d'un champ magnetique. J. de. Phys. (Paris) 3, 393-415.

Dingle, H., 1949. Universal principles. Nature 164, 163-165.

Dubois, J., Novaili, S., 1989. Quantification of the fracturing of the slab using a fractal approach. Earth Planet. Sci. Lett. 94, 97-108.

Eigen, M., Winkler, R., 1975. Das Spiel. R. Piper & Co. Verlag, Munchen.

Eneva, M., 1996. Effect of limited data sets in evaluating the scaling properties of spatially distributed data: An example from mining-induced seismic. Geophys. J. Int. 124, 773-786.

Enya, O., 1901. On aftershocks. Rep. Earthq. Inv. Comm. 35, 35-56. (in Japanese)

Frohlich, C., 1989. The nature of deep-focus earthquake. Annu. Rev. Earth Planet. Sci. 17, 227-254.

Grassberger, P., 1983. Generalized distributions of strange attractors. Phys. Lett. 97, 227-230.

Guo, Z., Ogata, Y., 1995. Correlation between characteristic parameters of aftershock distributions in time, space and magnitude. Geophys. Res. Lett. 22, 993-996.

Guo, Z., Ogata, Y., 1997. Statistical relations between the parameters of aftershocks in time, space and magnitude. J. Geophys. Res. 102, 2857-2873.

Gutenberg, B., Richter, C.F., 1954. Seismicity of the Earth. Princeton Univ. Press, Princeton.

Hatori, T., 1963. Directivity of tsunami. Bull. Earthquake Res. Inst. 41, 61-81.

Hatton, C.G., Main, I.G., Meredith, P.G., 1993. A comparison of seismic and structural measurements of scaling exponents during tensile subcritical crack growth. J. Struct. Geol. 15, 1485-1495.

Hirata, T., 1986. Omori's power law for aftershocks and fractal geometry of multiple fault system. Zishin (J. Seismol. Soc. Jpn.) 39, 478-481. (in Japanese)

Hirata, T., 1987. Omori's power law aftershock sequences of microfracturing in rock fracture experiment. J. Geophys. Res. 92, 6215-6221.

Hirata, T., 1989a. A correlation between b-value and the fractal dimension of earthquakes. J. Geophys. Res. 94, 7507-7514.

Hirata, T., 1989b. Fractal dimension of fault systems in Japan: Fractal structure in rock

fracture geometry at various scales. Pure Appl. Geophys. 131, 157-170.

Hirata, T., Satoh, T., Ito, K., 1987. Fractal structure of spatial distribution of microfracturing in rock. Geophys. J. R. astr. Soc. 90, 369-374.

Hosono, K., Yoshida, A., 1991. On the distribution of epicentral distance between the largest aftershock and the main shock. Zishin (J. Seismol. Soc. Jpn.) 44, 259-261. (in Japanese)

Hough, S.E., Jones, L.M., 1997. Aftershocks: Are they earthquakes or afterthoughts? EOS Trans. Am. Geophys. Union 78, 505.

Huang, J., Turcotte, D.L., 1988. Fractal distributions of stress and strength and variations of b-value. Earth Planet. Sci. Lett. 91, 223-230.

Hwa, T., Kardar, M., 1989. Dissipative transport in open system: An investigation of self-organized criticality. Phys. Rev. Lett. 62, 1813-1816.

Iida, K., 1965. Earthquake magnitude, earthquake fault, and source dimensions. J. Earth Sci. Nagoya Univ. 13, 115-132.

Ishikawa, Y., 1986. SEIS-PC: New version. Geol. Data Process. 11, 65-74.

Ishikawa, Y., Mochizuki, E., Sakuma, K., Yamamoto, M., Naruto, N., 1989. Compile of focal mechanism solutions. Gekkan Chikyu (Earth Monthly) 3, 219-223. (in Japanese)

Ito, K., 1992. Towards a new view of earthquake phenomena. Pure Appl. Geophys. 138, 531-548.

Ito, K., Matsuzaki, M., 1990. Earthquakes as self-organized critical phenomena. J. Geophys. Res. 65, 6853-6860.

Jaeger, F.M., 1920. Lectures on the Principle of Symmetry and Its Application in All Natural Sciences 2nd Ed. Elsevier, Amsterdam.

Jensen, H.J., 1998. Self-organized Criticality: The Emergent Complex Behavior in Physical and Biological Systems. Cambridge Lect. Notes Phys. 10, Cambridge Univ. Press, Cambridge.

Kagan, Y., 1992. Seismicity: Turbulence of solid. Nonlinear Sci. Today. 2, 2-13.

Kagan, Y., Knopoff, L., 1978. Statistical study of the occurrence of shallow earthquakes. Geophys. J. R. astr. Soc. 55, 67-86.

Kagan, Y., Knopoff, L., 1980. Spatial distribution of earthquakes, the two-point correlation function. Geophys. J. R. astr. Soc. 62, 303-320.

Kanamori, H., Allen, C.R., 1986. Earthquake repeat time and average stress drop. In: Das, S., Boatwright, J., Scholz, C.H. (Eds.), Earthquake Source Mechanics. AGU Monogr. 37, Am. Geophys. Union, Washington D.C., pp. 227-235.

Kanamori, H., Anderson, D.L., 1975. Theoretical basis of some empirical relations in seismology. Bull. Seismol. Soc. Am. 65, 1073-1095.

King, G., 1983. The accommodation of large strains in the upper lithosphere of the earth and other solids by self-similar fault systems: The geometric origin of b-value. Pure Appl. Geophys. 121, 761-815.

Kisslinger, C., 1996. Aftershocks and fault-zone properties. Adv. Geophys. 38, 1-36.

Kisslinger, C., Jones, L.M., 1991. Properties of aftershocks in southern California. J. Geophys. Res. 96, 11947-11958.

Korvin, G., 1992. Fractal Models in the Earth Sciences. Elsevier, Amsterdam.

Koyama, J., 1994. Stochastic scaling and relaxation of earthquake activities. In: Ouchi, T. (Ed.), Mathematical Seismology (8). Inst. Statist. Math., Tokyo, pp. 1-6.

Koyama, J., 1997. The Complex Faulting Process of Earthquakes. Modern Approaches Geophys. 16, Kluwer Acad. Pub., Dordrecht, Netherlands.

Main, I.G., 1996. Statistical physics, seismogenesis, and seismic hazard. Rev. Geophys. 34, 433-462.

Main, I.G., Burton, P.W., 1984. Information theory and the earthquake frequency-magnitude distribution. Bull. Seismol. Soc. Am. 74, 1409-1426.

Main, I.G., Meredith, P.G., Jones, C., 1989. A reinterpretation of the frequency seismic b-value anomaly from fracture mechanics. Geophys. J. 96, 131-138.

Main, I.G., Peacock, S., Meredith, P.G., 1990. Scattering attenuation and the fractal geometry of fracture systems. Pure Appl. Geophys. 133, 283-304.

Malin, P.E., Blakeslee, S.N., Alvarez, M.G., Martin, A.J., 1989. Microearthquake imaging of the Parkfield asperity. Science 244, 557-559.

Mandelbrot, B.B., 1983. The Fractal Geometry of Nature. W. H. Freeman and Company, New York.

Matsuda, T., 1977. Estimation of future destructive earthquakes from active faults on land in Japan. J. Phys. Earth, Suppl. 25, 251-260.

Merceron, T., Velde, B., 1991. Application of Cantor's method for fractal analysis of fractures in the Toyoha mine, Hokkaido, Japan. J. Geophys. Res. 96, 16641-16650.

Mikumo, T., Miyatake, T., 1979. Earthquake sequences on frictional fault model with non-uniform strengths and relaxation times. Geophys. J. R. astr. Soc. 59, 497-522.

Mogi, K., 1962. On the time distribution of aftershocks accompanying the recent major earthquakes in and near Japan. Bull. Earthquake Res. Inst. 40, 107-124.

Mogi, K., 1967. Regional variation of aftershock activity. Bull. Earthquake Res. Inst. 45, 711-725.

Mogi, K., 1985. Earthquake Prediction. Acad. Press, Tokyo.

Nagahama, H., 1991. Fracturing in the solid earth. Sci. Reps. Tohoku Univ., 2 (Geol.) 61, 103-126.

Nagahama, H., 1994. Self-affine growth pattern of earthquake rupture zones. Pure Appl. Geophys. 142, 263-271.

Nagahama, H., 2000. Fractal scalings of rock fragmentation. Earth Sci. Frontiers. 7, 169-177.

Nagahama, H., Teisseyre, R., 1998. Micromorphic continuum, rotational wave and fractal properties of earthquakes and faults. Acta Geophys. Pol. 46, 277-294.

Nagahama, H., Teisseyre, R., 2000a. Micromorphic continuum and fractal fracturing in the lithosphere. Pure Appl. Geophys. 157, 559-574.

Nagahama, H., Teisseyre, R., 2000b. Micromorphic continuum and fractal properties of faults and earthquakes. In: Teisseyre, R., Majewski, E. (Eds.), Earthquake Thermodynamics and Phase Transformations in the Earth's Interior. Int. Geophys. 76, Acad. Press, San Diego, pp. 425-440.

Nagahama, H., Yoshii, K., 1994. Scaling laws of fragmentation. In: Kruhl, J.H. (Ed.), Fractals and Dynamical Systems in Geosciences. Springer-Verlag, Berlin, pp. 25-36.

Nagy, D., 1990. Manifesto on (dis)symmetry with some preliminary symmetries.

Symmetry: Culture and Science 1, 3-26.

Nagy, D., 1996. The western symmetry and the Japanese katachi shake hands: Interdisciplinary study of symmetry and morphological science (Formology). In: Ogawa, T., Miura, K., Masunari, T., Nagy, D. (Eds.), KATACHI ∪ SYMMETRY. Springer-Verlag, Tokyo, pp. 27-46.

Nakamura, N., Nagahama, H., 2000. Curie symmetry principle: Does it constrain the analysis of structural geology. In: Ogawa, T., Mitamura, S., Nagy, D., Takaki, R. (Eds.), Proc. 2nd Int. KATACHI ∪ SYMMETRY Symp. Forma 15, 87-94.

Nakamura, N., Otsuki, K., Nagahama, H., 1996. A spring-network model of fault-system evolution. In: Paor D. G D. (Ed.), Structural geology and personal computers. Pergamon, pp. 343-358.

Nanjo, K., Nagahama, H., 2000. Spatial distribution of aftershocks and the fractal structure of active fault systems. Pure Appl. Geophys. 157, 575-588.

Nanjo, K., Nagahama, H., Satomura, M., 1998. Rates of aftershock decay and the fractal structure of active fault systems. Tectonophysics 287, 173-186.

Nanjo, K., Nagahama, H., Yodogawa, E., 2000. Symmetry properties of spatial distribution of microfracturing in rock. In: Ogawa, T., Mitamura, S., Nagy, D., Takaki, R. (Eds.), Proc. 2nd Int. KATACHI ∪ SYMMETRY Symp. Forma 15, 95-101.

Nicolis, G., Prigogine, I., 1977. Self-organization in Nonequilibrium Systems: From Dissipative Structures to Order through Fluctuations. John Wiley & Sons, New York.

Ogata, Y., 1988, Statistical model for earthquake occurrences and residual analysis for point processes. J. Am. Stat. Assoc. 83, 9-27.

Ohtsuka, M., Kara, R., Minami, T., 1985. On relaxation law for aftershocks. In: Takahashi, H. (Ed.), A Synthetic Investigation on Activity and Disasters of 1984 Shimabara Earthquake Swarm. The Ministry of Education, Japan, pp. 67-73. (in Japanese)

Okubo, P.G., Aki, K., 1987. Fractal geometry in the San Andreas fault system. J. Geophys. Res. 92, 345-355.

Omori, F., 1894. On the aftershocks of earthquake. J. Coll. Sci. Imp. Univ. Tokyo 7, 111-200.

Oncel, A.O., Alptekin, O., Main, I.G., 1995. Temporal variations of the fractal properties of seismicity in the western part of the North Anatolian fault zone: Possible artifacts due to improvements in station coverage. Nonlinear Proc. Geophys. 2, 145-157.

Otsuka, M., 1964. Earthquake magnitude and surface fault deformation. J. Phys. Earth 12, 19-24.

Otsuki, K., 1998. An empirical evolution law of fractal size frequency of fault population and its similarity law. Geophys. Res. Lett. 25, 671-674.

Palmer, A.R., 1986. Inferring relative levels of genetic variability in fossils: The link between heterozygosity and fluctuating symmetry. Paleobiology 12, 1-5.

Palmer, A.R., Strobeck, C., 1986. Flictuating asymmetry: Measurement, analysis, patterns. Ann. Rev. Ecol. Syst. 17, 391-421.

Ranalli, G., 1987. Rheology of the Earth: Deformation and Flow Processes in Geophysics and Geodynamics. Allen & Unwin, Boston.

Richter, C.F., 1958. Elementary Seismology. H. Freeman and Co., San Francisco.

Rosen, J., 1995. Symmetry in Science: An Introduction to the General Theory. Springer-Verlag, New York.

Sadovisky, M.A., Golubeva, T.V., Pisarenko, V.F., Shnirman, M.G., 1984. Characteristic dimensions of rock and hierarchical properties of seismicity. Izv. Acad. Sci. USSR Phys. Solid Earth 20, 87-96 (English translated from Characteristic rock dimensions and hierarchy properties of seismicity. Fizika Zemli No. 2, 3-15, 1984).

Sato, R., Abe, K., Okada, Y., Shimazaki, K., Suzuki. Y., 1989. Handbook of faulting parameters of earthquakes in Japan. Kashima Shuppan, Tokyo. (in Japanese)

Sattinger, D.H., 1978. Group representation theory, bifurcation theory and pattern formation. J. Funct. Anal. 28, 58-101.

Scholz, C.H., 1968. Microfractures, aftershocks, and seismicity. Bull. Seismol. Soc. Am. 58, 1117-1130.

Scholz, C.H., Aviles, C.A., 1986. The fractal geometry of faults and faulting. In: Das, S., Boatwrigrt, J., Scholz, C.H. (Eds.), Earthquake Source Mechanics. Maurice Ewing 6, Am. Geophys. Union, Washington, D.C., pp. 147-155.

Shaw, B.E., 1993. Generalized Omori law for aftershocks and foreshocks from a simple dynamics. Geophys. Res. Lett. 20, 907-910.

Shimazaki, T., Nagahama, H., 1995. Does earthquake break down irregularly?

Collective and individual properties of earthquakes. Kagaku (Science) 65, 241-256. (in Japanese)

Stanley, H.G., 1971. Introduction to Phase Transitions and Critical Phenomena. Claredon Press, Oxford.

Stewart, I., Golubitsky, M., 1992. Fearful Symmetry: Is God a Geometer? Blackwell Pub., London.

Stineman, R.W., 1980. A consistently well-behaved method of interpolation. Creat. Comp. 6, 54-57.

Takayasu, H., 1990. Fractals in the Physical Sciences. Manchester Univ. Press, New York.

Tang, C., Bak, P., 1988. Mean field theory of self-organized critical phenomena. J. Stat. Phys. 51, 797-802.

The Research Group for Active Faults of Japan, 1991. Active Faults in Japan: Sheet Maps and Inventories (Revised Ed.). Univ. of Tokyo Press, Tokyo. (in Japanese with English summary)

Tsuboi, T., 1956. Earthquake energy, earthquake volume, aftershock area, and strength of the earth 1 s crust. J. Phys. Earth 4, 63-66.

Turcotte, D. L., 1986a. Fractals and fragmentation. J. Geophys. Res. 91, 1921-1926.

Turcotte, D.L., 1986b. A fractal model for crustal deformation. Tectonophysics 132, 261-269.

Turcotte, D.L., 1989. Fractals in geology and geophysics. Pure Appl. Geophys. 131, 171-196.

Turcotte, D.L., 1992. Fractals and Chaos in Geology and Geophysics. Cambridge Univ. Press, New York.

Turcotte, D.L., 1997. Fractals and Chaos in Geology and Geophysics 2nd Ed. Cambridge Univ. Press, New York.

Turcotte, D.L., 1999. Self-organized criticality. Rep. Prog. Phys. 62, 1377-1429.

Utsu, T., 1957. Magnitude of earthquakes and occurrence of their aftershocks. Zishin (J. Seismol. Soc. Jpn.) 10, 35-45. (in Japanese)

Utsu, T., 1961. A statistical study on the occurrence of aftershocks. Geophys. Mag. 30, 521-605.

Utsu, T., 1962. On the nature of three Alaskan aftershock sequences of 1957 and 1958. Bull. Seismol. Soc. Am. 52, 279-297.

Utsu, T., 1969. Aftershocks and earthquake statistics (1): Some parameters which characterize an aftershock sequence and their interrelations. J. Fac. Sci. Hokkaido Univ., 7 (Geophys.) 3, 129-195.

Utsu, T., 1970. Aftershocks and earthquake statistics (2): Further investigation of aftershocks and other earthquake sequences based on a new classification of earthquake sequences. J. Fac. Sci. Hokkaido Univ., 7 (Geophys.) 3, 197-266.

Utsu, T., 1991. Seismology 2nd Ed. Kyoritsu Shuppan, Tokyo. (in Japanese)

Utsu, T., 1999. Seismicity Studies: A Comprehensive Review. Univ. of Tokyo Press, Tokyo. (in Japanese)

Van Valen, L., 1962. A study of fluctuating asymmetry. Evolution 16, 125-142.

Velde, B., Dubois, J., Tochard, G., 1991. Fractal patterns of fractures in granites. Earth

Planet. Sci. Lett. 104, 25-35.

Walsh, J.L., 1999. A closed set of normal orthogonal functions. In: Rivlin, T.J., Saff, E.B. (Eds.), Joseph L. Walsh Selected Papers. Springer-Verlag, New York, pp. 109-128 (Reprinted from A closed set of normal orthogonal functions. Am. J. Math. 45, 5-24, 1923).

Watanabe, K., 1986. Stochastic evaluation of the two dimensional continuity of fractures in a rock mass. Int. J. Rock Mech. Min. Sci. Geomech. Abstr. 23, 431-437.

Wells, D.L., Coppersmith, K.J., 1994. New empirical relationships among magnitude, rupture length, rupture area, and surface displacement. Bull. Seismol. Soc. Am. 84, 974-1002.

Whyte, L.L., 1949a. The Unitary Principle in Physics and Biology. Cresset Press, London.

Whyte, L.L., 1949b. Tendency towards symmetry in fundamental physical structures. Nature 163, 762-763.

Whyte, L.L., 1974. The Universe of Experience: A World View beyond Science and Religion. Harper & Row, New York.

Wiemer, S., Katsumata, K., 1999. Spatial variability of seismicity parameters in aftershock zones. J. Geophys. Res. 104, 13135-13151.

Yamashita, T., Knopoff, L., 1987. Models of aftershock occurrence. Geophys. J. R. astr. Soc. 91, 13-26.

Yodogawa, E., 1982. Symmetropy, an entropy-like measure of visual symmetry. Percept. Psychophys. 32, 230-240.

Yonekura, N., 1972. A review on seismic crustal deformations in and near Japan. Bull. Geograph. Inst. Univ. Tokyo 4, 17-50.

Yoshida, A., Mikami, N., 1986. Temporal and spatial distribution of aftershocks: A preliminary report. In: Saito, M. (Ed.), Mathematical Seismology. Inst. Statist. Math., Tokyo, pp. 98-108. (in Japanese)

Zabrodsky, H., Peleg, S., Avnir, D., 1992. Continuous symmetry measures. J. Am. Chem. Soc. 114, 7843-7851.

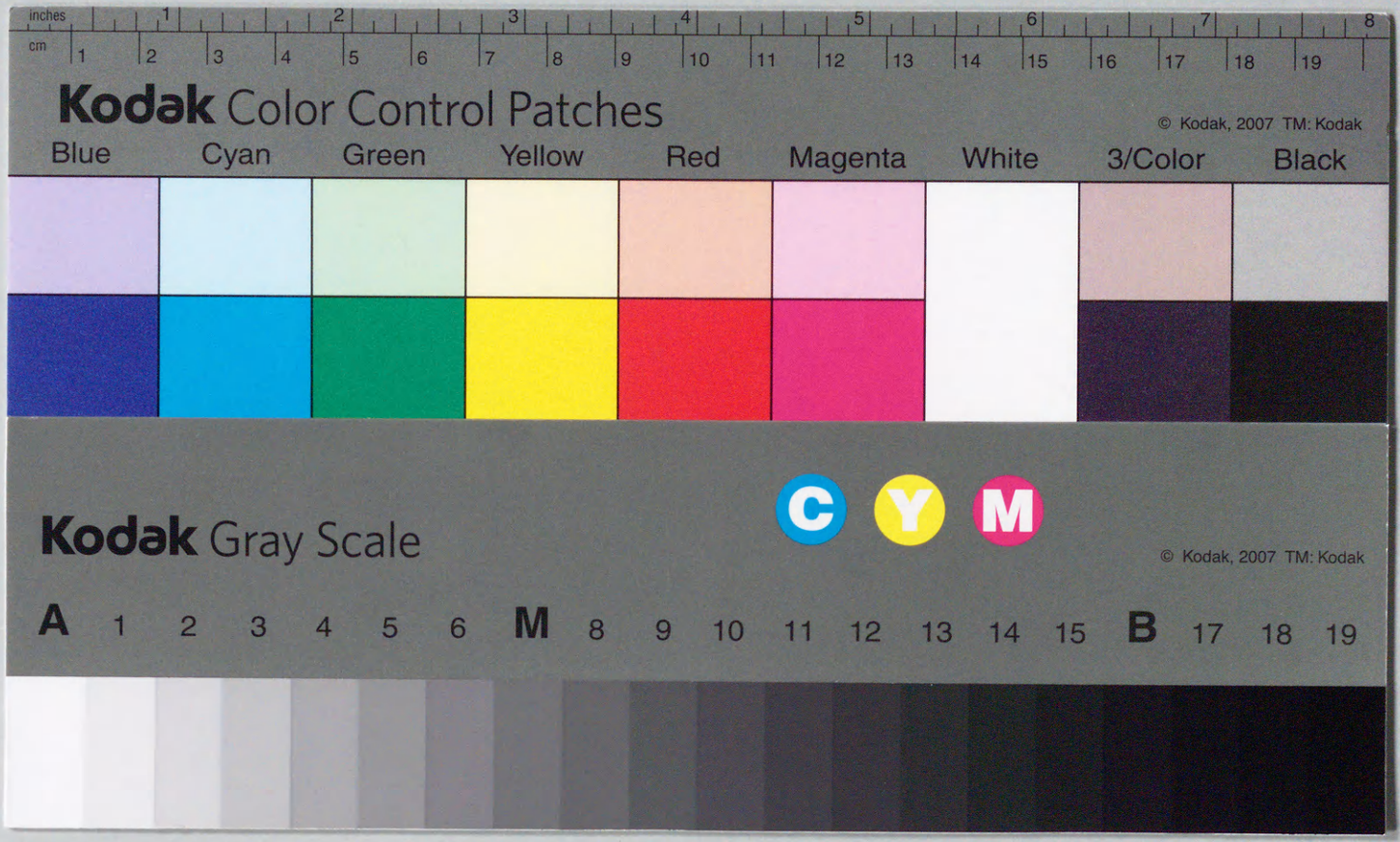
inches
cm
Kodak Color Control Patches
© Kodak, 2007 TM: Kodak
Blue
Cyan
Green
Yellow
Red
Magenta
White
3/Color
Black
Kodak Gray Scale
C
Y
M
© Kodak, 2007 TM: Kodak
A 1 2 3 4 5 6 M 8 9 10 11 12 13 14 15 B 17 18 19